Virial coefficients of helium-4 from ab initio based molecular models

Andrew J. Schultz and David A. Kofke*

Department of Chemical and Biological Engineering, University at Buffalo, The State University of New York, Buffalo, NY 14260-4200, USA

E-mail: kofke@buffalo.edu

April 13, 2019

Abstract

We examine the accuracy of virial coefficients $B_n(T)$ for ^{4}He for $n = 2$ to 7 and temperatures T from 20 K to 1000 K, while reporting new values from semiclassical and (for $n = 5$) path-integral Monte Carlo (PIMC) calculations. All coefficients are based on first-principles 2- and 3-body molecular models from the literature, and have estimated stochastic and systematic uncertainty between 0.005% to 20%, depending on n and T (almost all of this due to estimated inaccuracy in the 3-body model). The calculated $B_n(T)$ are used to examine the virial equation of state (VEOS) against experimental data from the literature, from 223.15 K to 500 K and pressures up to 38 MPa. First, the VEOS is used to calibrate the data, providing adjustments not exceeding the data's estimated systematic uncertainty. Then, findings from the comparison include: (1) the VEOS based on the *ab initio* $B_n(T)$ is fully consistent with the experimental data; (2) the series requires coefficients up to $n = 5$ in order to agree with experiment within all relevant uncertainties; (3) individual values $B_k(T)$ can be regressed accurately from the experimental data if other coefficients $B_n(T)$, $n \neq k$ are

given from the *ab initio* calculations; however, the uncertainty of these values is less than the coefficient magnitude only for $k \leq 5$.

Keywords: Mayer-sampling Monte Carlo; virial coefficients; helium

Introduction

Decades of steady advances in first-principles modeling of the electronic structure of molecular systems is reaching a point where these methods can yield computation-based data about not just individual molecules, but also bulk-system properties. It is hoped that eventually such data will come to be viewed as being more accurate and reliable than experiment, at least for certain classes of properties and substances.

One route to such an end is via computational cluster integrals. In this framework, thermodynamic properties are expressed via integrals over the configurations of two, three, four, etc. molecules, with an integrand that depends on the intermolecular potential. These integrals define coefficients that appear in density and mole-fraction series for the properties. The virial coefficients are the best-known example of such quantities, which yield the pressure via the virial equation of state (VEOS).[1–3] The VEOS is:

$$Z \equiv \frac{p}{\rho RT} = 1 + B_2(T)\rho + B_3(T)\rho^2 + \cdots + B_n(T)\rho^{n-1} + \ldots \tag{1}$$

Here, Z is the compressibility factor, which is defined in terms of the pressure p, molar density ρ, and temperature T; R is the gas constant. Also, $B_n(T)$ is the nth virial coefficient, and we will denote as VEOSn the series truncated after the term B_n. This framework is appealing because it provides a rigorous and direct connection between molecular interactions and thermodynamic properties. Further, it does so while considering the interactions of just a few molecules at a time, so its demands on electronic structure methods are as modest as they can possibly be, while still addressing bulk behavior.

Calculation of properties via computational cluster integrals is still severely limited in scope, particularly if the standards for accuracy are set by those available from experiment. However, capabilities are advancing rapidly. The boundary of what is possible may be pushed in any of several directions: (1) more accurate electronic-structure methods; (2) larger and more complex molecules; (3) molecular flexibility, and treatment of intramolecular degrees of freedom; (4) lower temperatures, where nuclear quantum effects are significant; (5) higher-order coefficients, requiring integrals over more molecules and thereby allowing application to higher densities; and (6) mixtures, introducing the need to model interactions between unlike molecules.

In the present work, we focus on helium-4 (^{4}He, CAS 7440-59-7), and generate results for coefficients to seventh order in density. We make use of very accurate molecular models from the literature, which are based on fits of high-quality *ab initio* two- and three-body potentials. We consider temperatures low enough to require attention to nuclear quantum effects, but not so low that a semiclassical treatment cannot be used. Thus, this work mainly advances the 5th item in this list of development directions, while also touching on the 1st and 4th. We build on results presented by us in a previous study,[4] where we reported ^{4}He virial coefficients $B_n(T)$ for $n = 2$ to 4 for temperatures from 2.6 K to 1000 K, using path-integral Monte Carlo (PIMC) for the very-low-temperature region. That study itself followed earlier work[5] by us for $n = 2$ to 5 from 50 K to 1000 K using a semiclassical treatment of nuclear quantum effects on the pair potential (with nonadditive contributions treated classically). At about the same time, Garberoglio[6] reported coefficients for $n = 2$ to 4 using a centroid approximation of the exact path-integral treatment of quantum effects. This approximation is similar to a semiclassical approach, but it allows handling of multibody quantum effects. Prior to this, Garberoglio and Harvey[7] reported coefficients for $n = 3$ at low temperatures, 2.6 K to 24.5561 K, with consideration of nuclear exchange (which they found to be significant below 7 K) and isotope effects (examining both ^{3}He and ^{4}He); these results were extended by them to higher temperatures and to compute the third acoustic virial coefficient as well.[8] All

of the foregoing studies employed the pair potential of Przybytek et al.[9,10] (which was first presented in 2010), and the (2009) three-body potential of Cencek et al.,[11] both of which are based on state-of-the-art *ab initio* calculations; these are also the potentials used for most of the coefficients reported here. However, while our study was in progress, Przybytek et al. reported[12] another pair potential, more accurate than the one presented in 2010. We have done calculations using this potential as well, albeit to a more limited extent. Calculations before 2009 are summarized in the report of the first *ab initio*-based calculation of B_3, which was published by Garberoglio and Harvey in that year.[13]

This development is motivated by interest in testing the best available experimental data for the equation of state of helium. There are two sources of data in particular,[14,15] each covering a different (but overlapping) range of temperatures. Comparisons to available first-principles-based virial coefficients finds an encouraging but imperfect degree of consistency. There is question as to whether observed discrepancies have to do with the shortcomings in the analysis of the experimental data, or to breakdown of the VEOS as it is pushed outside the range that can be accurately described with available coefficients. Knowledge of the coefficients reported here helps to resolve this question. There is a clear precedent for such a development, given that values of B_2 to B_5 computed from first-principles considerations have already been used to reduce uncertainties in values of B_4 as derived from analysis of experimental data.[5,15] We also give attention here to the question of accuracy of the computed coefficients, which we estimate using the reported accuracy of the *ab initio* pair potentials.

This paper is organized as follows. In the next section, we review the molecular models used to describe the interaction energy of the helium atoms, and we describe the methods used to calculate the virial coefficients from these models. We describe how we estimate the limits of accuracy of the computed coefficients, as propagated from the estimated accuracy of the potentials. We present our results and examine the relative magnitudes of the various sources and measures of the error in the coefficients. We then examine the virial equation

based on the computed coefficients, and analyze its performance in relation to experimental data. We finish with a summary and conclusions.

Models and Methods

Molecular models

In 2010 Przybytek et al.[9,10] introduced a very accurate pair potential by taking high-accuracy values[16,17] of the ^{4}He-^{4}He interaction energy in the Born-Oppenheimer approximation, and adding corrections for nuclear-electronic coupling, relativity, and quantum electrodynamics. In reporting the potential, Przybytek et al. computed coefficients for terms that capture the correct long-range asymptotic behavior, and used these as part of a functional form that was fit to 17 values of the He-He energy for separations ranging from 1 to 12 bohr. By examining the behavior with respect to the size of the electronic basis sets, they estimated the maximum inaccuracy of each term contributing to the potential, and reported this aggregated uncertainty as upper and lower bounds for the pair energy as a function of separation. In this manner Przybytek et al. estimated the accuracy of their potential to be within 0.02% of the total pair energy. The improved model reported by Przybytek et al.[12] in 2017 achieved an order-of-magnitude increase in the accuracy of the pair interaction energy. This was accomplished primarily through a better treatment of the full 4-electron Born-Oppenheimer wave function, but also with more attention to the adiabatic and relativistic contributions.

Nonadditive contributions to the energy of the ^{4}He trimer at its energy minimum amount to about 0.3% of the total interaction energy,[11] which is significant on the scale of the accuracy of the pair potential. Cencek et al.[11] developed a functional form for this contribution by fitting 253 trimer configurations using the full-configuration-interaction method. They estimated the accuracy of their model to be within 2% of the total non-additive contribution, or 0.007% of the total trimer potential. Inaccuracy of even this small size is significant relative to the precision of our calculations, so in this study we estimate how this uncertainty

propagates to the values of the virial coefficients.

The mass of the helium atom is small, and consequently any calculation of its properties must take into account nuclear quantum effects. Complete neglect of these contributions (i.e., a fully classical treatment) introduces an error of at least 1% in the value of B_4 for all temperatures up to at least 1000 K.[4] While rigorous handling of nuclear quantum effects can be accomplished using PIMC, in some cases we employ a more approximate semiclassical treatment. In particular, in most of our calculations the He-He interaction is given by a quadratic Feynman-Hibbs modification of the pair potential, $u(r)$ (where r is the pair separation):

$$u^{\mathrm{QFH}}(r) = u(r) + \frac{\hbar^2}{24 k_{\mathrm{B}} T (m/2)} \left[\frac{\partial^2 u}{\partial r^2} + \frac{2}{r} \frac{\partial u}{\partial r} \right], \tag{2}$$

where $\hbar$ is the reduced Planck constant, k_{B} is the Boltzmann constant, and m is the mass of a ^{4}He atom. In principle, the three-body potential should be modified similarly, but given its complexity and considering its smaller contribution to the energy, we neglect such effects.

In addition, we report new values of $B_5(T)$ from PIMC calculations, from 2.6 K to 1000 K, and some low-temperature $B_2(T)$ PIMC results. These were performed as described in our 2012 paper[4] reporting PIMC values for $B_2(T)$, $B_3(T)$, and $B_4(T)$. These new PIMC data were computed shortly after the 2012 work was published, and are reported here for the first time. These values do not include effects of quantum statistics (nuclear exchange), which for ^{4}He are significant below approximately 5 K.[7]

Computational details

All virial coefficients reported here were computed using the Mayer-sampling Monte Carlo method,[18] wherein the coefficient B_n is given via a calculation involving n He atoms. This method applies Metropolis Monte Carlo[19,20] to average the sum of cluster integrals that defines each coefficient, using importance sampling based on the value of the integrand defined by the cluster sum (with accommodation made for the possibility of a negative

integrand value). We use the recursion due to Wheatley[21] to compute the cluster integrand; this algorithm has been recently shown[22] to apply to multibody potentials in addition to the pairwise-additive forms considered in its original development. The MSMC calculation yields the ratio of the desired integral to the value for a known reference system. For each virial coefficient, the reference integral was given as the virial coefficient of the same order but for a system of hard spheres[23] (HS); the HS diamter (in Angstroms) was taken to be $3.0 + 120/(100 + T/\mathrm{K})$ when computing 3-body contributions and $2.4 + 120/(100 + T/\mathrm{K})$ for computing 2-body contributions, except that it was 3.0 when not computing the difference from the Percus-Yevick solution (see below). Overlap sampling[24,25] was employed to eliminate any possible bias in the computed values that might result from systematic neglect of relevant configurations.

Each virial coefficient was computed as a sum of four contributions, as follows:

$$\begin{aligned} B_n(T) = &[B_n(T;2a)] + [B_n(T;2) - B_n(T;2a)] + [B_n(T;2a3a) - B_n(T;2a)] \\ &+ [B_n(T) - B_n(T;2) - B_n(T;2a3a) + B_n(T;2a))] \end{aligned} \tag{3a}$$

The modifiers α on $B_n(T;\alpha)$ indicate various approximations to the potential model: "2" and "3" indicate, respectively, the presence of semiclassical 2- and classical 3-body contributions to the potential; an "a" indicates the use of a form of the potential contribution that is approximate but more quickly computed. The absence of any modifiers indicates the coefficient with the full and accurate 2- and 3-body contributions.[9,11] Each term in square brackets was computed using its own MSMC simulation, and the breakdown of the coefficient this way is designed to allow the calculations involving the more computationally expensive potentials to be obtained as a small difference from an approximate value. Additionally, for $n = 2$ to 5, contributions involving 2-body interactions only (2/2a) employed an additional

separation:

$$B_n(T;2/2a) = B_n^{\rm PY}(T;2/2a) + \big(B_n(T;2/2a) - B_n^{\rm PY}(T;2/2a)\big) \tag{3b}$$

Here $B_n^{\rm PY}$ is the virial coefficient as given by Percus-Yevick (PY) theory,[26] and this can be computed directly with no uncertainty. The remaining difference can be introduced in terms of the graphs appearing in B_n that are not in $B_n^{\rm PY}$; for $n = 2$ and 3, this difference is zero. For $n = 6$ and 7, $B_n(T)$ was computed just using the breakdown given in Eq. (3a).

The computation time devoted to each part (number of simulations and number of steps for each simulation) was allocated so as to minimize the difficulty[27] of the overall calculation.[4] For each temperature, approximately 50 hours of central processing unit (CPU) time were used to compute semiclassical values of B_3, B_4 and B_5, approximately 80 CPU-hours for B_6 and 160 CPU-hours for B_7. All calculations were performed with the Etomica molecular modeling package.[28] Uncertainties for each contribution were computed based on block averages in each simulation with the overall uncertainty computed by propagating the uncertainty through the sum in Eq. (3). All uncertainties are reported as one standard deviation of the mean, i.e., at 68% level of confidence.

Accuracy estimation

Inaccuracies in the helium pair and trimer potentials propagate to introduce inaccuracy in the virial coefficients computed from them, and from there to pressures computed using the VEOS. It is difficult to estimate this propagated inaccuracy in a rigorous way, even with good estimates of the accuracy of the interatomic potentials. Nevertheless, it is worthwhile to attempt such estimates, because they can be valuable in guiding the application of the computed coefficients to the analysis of experimental data, and in reconciling differences between computation and experiment. This information can also be used to assess the accuracy of quantities derived from the equation of state, such as Boltzmann's constant.[29]

Przybytek et al.[9,10,12] provide estimates of the accuracy of their 2010 potential in the form of conservative error bounds on the pair energy, as a function of separation. The 2017 potential has an estimated error that is about ten times smaller than that for the 2010 potential. Our virial coefficients are based on the latter (i.e., the 2010 model), but to better assess the effect, we examine error propagation for both. In addition, we estimate the difference in the coefficients when using one potential versus the other.

Cencek et al.[11] estimate the accuracy of their 3-body potential to be 2% of the 3-body contribution for each trimer configuration. This too appears to be a conservative estimate, as it bounds the 1.9% relative uncertainty that they compute for the minimum-energy trimer configuration. Following Garberoglio and Harvey,[8] we interpret the 2% relative uncertainty as an expanded ($k = 2$) uncertainty; to be consistent with the use of standard ($k = 1$) uncertainties for other quantities involved in this study, we consider the propagation of a 1% shift in the 3-body contribution when assessing its effect on the virial coefficients.

Propagation of inaccuracy to B_2 is straightforward, because any up/down shift in a given part of the pair potential corresponds directly to an up/down shift in the value of B_2. For B_3 and higher, the connection is not nearly so simple. Shifts in the potential can have effects on B_3, B_4, etc. that go in either direction, because of the complicated dependence of the sign of the integrand on all the pair interactions in the cluster sum. Moreover, shifts in one part of the potential can lead to a change in the coefficient in one direction, and the same shift in another part of the potential can have the opposite effect. Compounding this is the differing effects that potential shifts may have on different coefficients in the virial series, so the net effect on the pressure will be even more uncertain. Finally, we should not expect that any estimates of the inaccuracy in the potential would apply to it uniformly; the potential may be biased in a positive direction at one value of the separation, and in a negative direction at another. In calculating the third virial coefficient of argon from a first-principles model, Cencek et al.[30] applied a very conservative criterion for estimating the inaccuracy in the third virial coefficient, considering for each configuration the maximum effect that inaccuracy in

the potential could have on the coefficient. This is not feasible for higher-order coefficients, so we do not attempt this here.

In light of the complications described above, and without detailed information about correlations in the inaccuracy for different separations, the best we can do with accuracy bounds on the potential is to see how much they affect the virial coefficients when the potential is shifted up by the estimated amount. Thus, if $\delta u > 0$ is the sum of absolute values of the estimates of the 2- and 3-body inaccuracies for a given configuration of atoms, we estimate the systematic uncertainty in B_n due to this via:

$$u^{\rm sys}(B_n) \equiv |B_n[u + \delta u] - B_n[u]| \tag{4}$$

We can calculate this effect most efficiently by computing directly the change in the coefficient with the shift in the potential. For each configuration of the cluster of He atoms, we compute the difference in the virial-coefficient integrand obtained upon shifting the 2- and 3-body contributions in the same direction by their $k = 1$ uncertainties. We then average this quantity as in any other MSMC calculation, yielding $u^{\rm sys}(B_n)$ via a single average. Direct calculation of the difference this way is much more efficient than computing the perturbed and unperturbed coefficients and differencing afterwards.

Additionally, we examine several measures of the sensitivity of the virial coefficients to inaccuracy in the pair potential only. Here, we use the PY approximation to compute the effect of changes in the pair potential on $B_n(T)$. The PY framework for this calculation has been presented elsewhere.[26] The approach considers only the pairwise contribution to B_n, and employs a classical treatment. The usefulness of the calculation assumes that the functional dependence of these approximate coefficients on the potential will mimic the dependence of the exact coefficients. We consider three quantities in particular. First, we estimate the effect of the estimated systematic error in the 2010 potential,[9,10] via:

$$u^{\rm sys}(2010) \equiv \left|B_n^{\rm PY}[u_{2010} + \delta u_{2010}] - B_n^{\rm PY}[u_{2010}]\right|, \tag{5a}$$

where u_{2010} indicates the 2010 pair potential, and δu_{2010} is its estimated systematic error. We do the same for the 2017 potential[12] (with definitions analogous to Eq. (5a)):

$$u^{\mathrm{sys}}(2017) \equiv \left| B_n^{\mathrm{PY}}[u_{2017} + \delta u_{2017}] - B_n^{\mathrm{PY}}[u_{2017}] \right| . \tag{5b}$$

Finally, we look at the difference in B_n between the two potentials:

$$\Delta B_n \equiv \left| B_n^{\mathrm{PY}}[u_{2017}] - B_n^{\mathrm{PY}}[u_{2010}] \right| . \tag{5c}$$

Results and Discussion

Coefficients

The calculated virial coefficients are reported in Tables 3 to 8 and displayed together in reduced form in Fig. 1. We report new semiclassical values for $n = 3$ to 7, in some cases improving on the precision of the values for $n = 3$ to 5 reported in Ref. 5. We also report values based on path-integral Monte Carlo (PIMC) for a more rigorous treatment of nuclear quantum effects (but excluding exchange). The PIMC results for $n = 3$ and 4 are the same as those reported previously,[4] and are presented here for convenience. Additionally, we report previously unpublished PIMC results for $n = 5$; these were computed using the methods and protocols described in Ref. 4. Finally, for $n = 4$ to 7 we present values determined using the PY approximation outlined in the previous section (PY is exact for $n = 2$ and 3), as applied to the semiclassical 2-body potential (PY does not accommodate 3-body interactions). Comparison of the approximate PY results to the correct values determined from MSMC allows us to gauge the reliability of the PY treatment, when used as in Eq. (5).

The coefficients in Fig. 1 are made dimensionless by a reference density, selected such that the reduced values are all of roughly the same order of magnitude. The reduced coefficients represent the contribution to the pressure at the reducing density, so a comparison of their

magnitudes at different temperatures gives an indication of how well the series is converged at this density. We use $\rho_r = 0.09$ mol/cm^3 as the reducing density, which is, to provide scale, about 5 times the experimental critical density (0.0172 mol/cm^3). We observe from the figure that for this density the series is converged at B_5 at the highest temperature ($T = 1000$ K), and that B_7 appears to be sufficient for temperatures as low as 100 K (this determination of course depends on the desired accuracy). We note that these temperatures are well above the ^{4}He critical temperature, which is 5.2 K.[31]

We have developed empirical fits of the coefficients as a function of temperature, to provide a convenient representation for various applications. We use the following form:

$$B_n^{\rm fit}(T) = \sum_{k=0}^{k_{\rm max}} \frac{a_k}{T^{ck}} \tag{6}$$

The set of coefficients $\{a_k\}$ and the constant c are used as fitting parameters for each virial coefficient B_n, and $k_{\rm max}$ is selected for each to provide a fit that describes the data to within their stochastic uncertainties, without overfitting (based on the χ^2 statistic). Values of the fitting coefficients are reported in Table 1.

Additionally, fits of the systematic uncertainties are given in the Supporting Information.

Table 1: Coefficients in temperature fit of ^{4}He virial coefficients, as given by Eq. (6) for T in kelvin and $B_n^{\rm fit}$ in (cm$^3\cdot$ mol^{-1})$^{n-1}$. Fits are valid for $20 \le T/{\rm K} \le 1000$. Fitted virial coefficients are based on PIMC for $n = 2$ to 5, and semiclassical for $n = 6$, 7.

	Virial coefficient order, n					
	2	3	4	5	6	7
c	0.1	0.3	0.35	0.3	0.55	0.75
a_0	338.57140836	9.592327	102.35818	2008.8372	-707.89	-33.7
a_1	-4191.20272117	-726.605907	-5012.31179	-74256.530	221323.21	1.7036269×10^6
a_2	22171.77401119	14874.392598	51159.6149	1.291883817×10^6	-2.888320019×10^7	-7.802339447×10^8
a_3	-65564.86849845	-61660.52365	483562.5028	-1.4378063154×10^7	1.0893029708×10^9	$3.3929183492\times10^{10}$
a_4	118093.5568359	127518.07691	-4.2150095260×10^6	9.5836800518×10^7	$-1.02598170698\times10^{10}$	$-3.88728250657\times10^{11}$
a_5	-129094.8165957	-184650.87946	1.5776087138×10^7	-3.3269356857×10^8	$5.81015803094\times10^{10}$	$2.426026819737\times10^{12}$
a_6	79428.5681979	256161.4697	-3.3411188756×10^7	6.3229199758×10^8	$-1.24096906209\times10^{11}$	—
a_7	-21569.771812	-170207.3826	2.9910922933×10^7	-5.1999615194×10^8	—	—

Error analysis

Various measures of the accuracy and precision of the coefficients are presented in Figs. 2 to 7, with points showing $1\%|B_n|$ to provide scale. These plots show that nuclear quantum effects and 3-body contributions to the potential dominate all other effects related to accuracy and precision. When both of these contributions are included (which we do), the remaining inaccuracies in the virial coefficients start as an amount on the order of 0.01% for $B_2(T)$ (which has no 3-body error contribution), and steadily grows relative to the coefficient value with increasing n: 0.15%, 0.5%, 2.2%, 5.8%, and 20% for n from 3 to 7, respectively, at 300 K—these ratios change significantly with temperature, mainly due to variation of the coefficient value. The largest contributor to the uncertainty in $B_n(T)$, $n \geq 3$, at all conditions is the systematic uncertainty in the 3-body contribution to the potential; stochastic errors are completely negligible in comparison. The importance of 3-body effects grows relative to the magnitude of the coefficient with increasing temperature, and accordingly the relative uncertainty contributed by the 3-body potential does as well. Also, as temperature increases, the correction for nuclear quantum effects given by PIMC in excess of SC stays in a roughly constant proportion to the magnitude of the coefficient, while decreasing in absolute size. These observations suggest that for $n = 6$ and 7, while the use of the semiclassical treatment (rather than PIMC) contributes significant error, it is likely to be exceeded by the effect of uncertainty in the 3-body potential.

The figures also present estimates of inaccuracy as propagated from inaccuracies in the pair potential, $u^{\text{sys}}(2010)$, $u^{\text{sys}}(2017)$, and ΔB_n in Eq. (5). These quantities are based on a classical treatment of the potential (as well as the PY approximation), but inasmuch as they are computed as differences, this approximation should not be very serious (we checked this for B_2 and find that the difference in $u^{\text{sys}}(2010)$ computed using semiclassical and classical treatments is indeed negligible). For $n = 2$, these inaccuracies are significantly larger than the uncertainty in the PIMC results, but they are still a small fraction of the coefficient value, ranging from 0.1% of B_2 at $T = 20$ K to 0.01% at $T = 1000$ K. For larger n, the

inaccuracy mostly remains less than 0.01% of the coefficient value, and becomes comparable to and then smaller than the stochastic uncertainties with increasing n (reflecting an increase in the stochastic uncertainties relative to the size of the coefficient). It is in all cases eclipsed by the uncertainty originating from the 3-body potential.

In general, the largest inaccuracy measure originating in the pair interaction is $u^{\mathrm{sys}}(2010)$, propagated from the estimated inaccuracy in the 2010 potential. Given that ΔB_n is much smaller, meaning the 2010-potential result does not differ that much from the 2017 potential, and given that $u^{\mathrm{sys}}(2017)$ is also small, it appears that $u^{\mathrm{sys}}(2010)$ is a significant overestimate of the inaccuracy.

Finally, the figures present the uncertainty in the respective coefficients when regressed from experimental data, as described below. For a given coefficient, this regression is performed assuming all other coefficients are known from the *ab initio* computed values. The primary source of the uncertainty represented by these points is the stochastic uncertainty in the experimental data, so it gives an idea of the best precision possible for evaluation of the virial coefficients from experiment. More details are given in the next section.

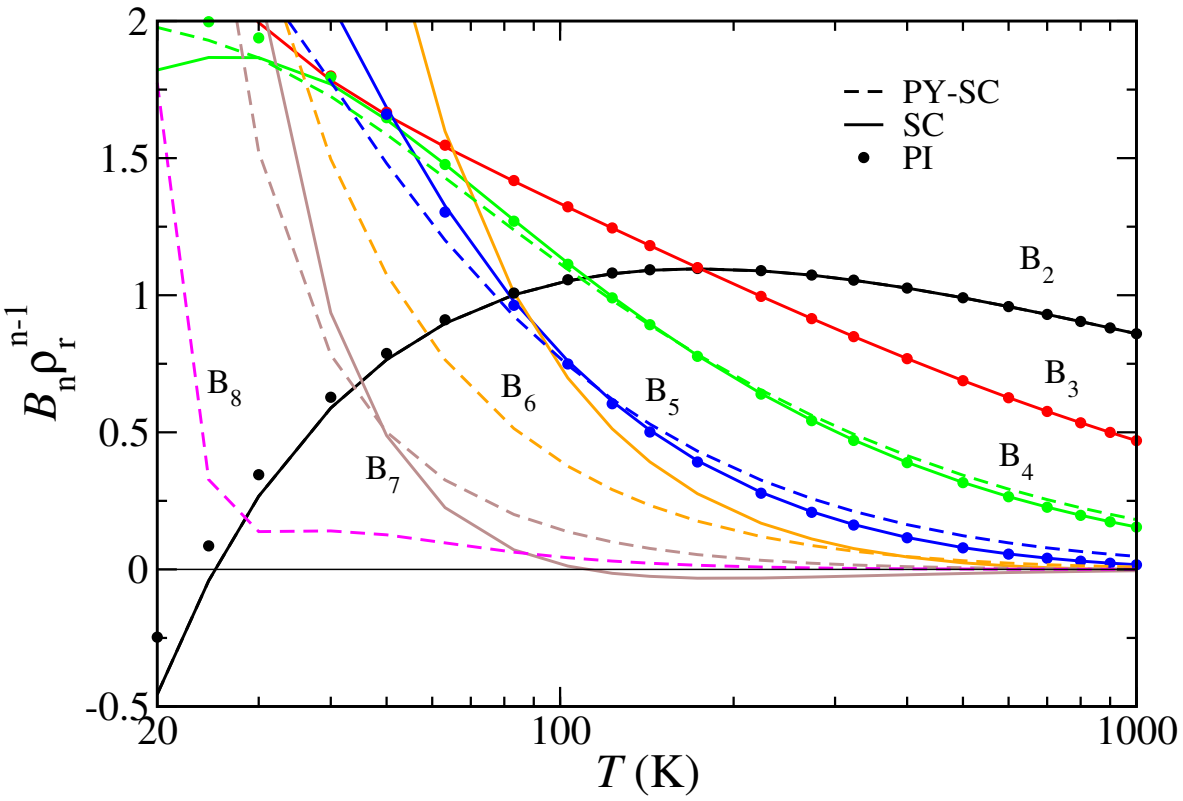

Figure 1: Virial coefficients $B_n(T)$ of ^{4}He, for $n = 2$ to 8 as computed from the semiclassical modification (Eq. (2)) of the 2010 pair potential of Pryzybek et al.[9,10] with three-body contributions from the 2009 potential of Cencek et al.[11] All coefficients are made dimensionless by a reference density $\rho_r = 0.09$ mol/cm^3. Filled circles are values from path-integral (PI) calculations reported previously[4] (n = 2-4) or new here ($n = 5$). Solid lines (SC) show computed semiclassical values . Dashed lines (PY-SC) are semiclassical results based on the PY approximation and the 2010 pair potential (without any 3-body contributions). All lines are drawn as straight line segments joining points (not shown) at the same temperatures as the PI results.

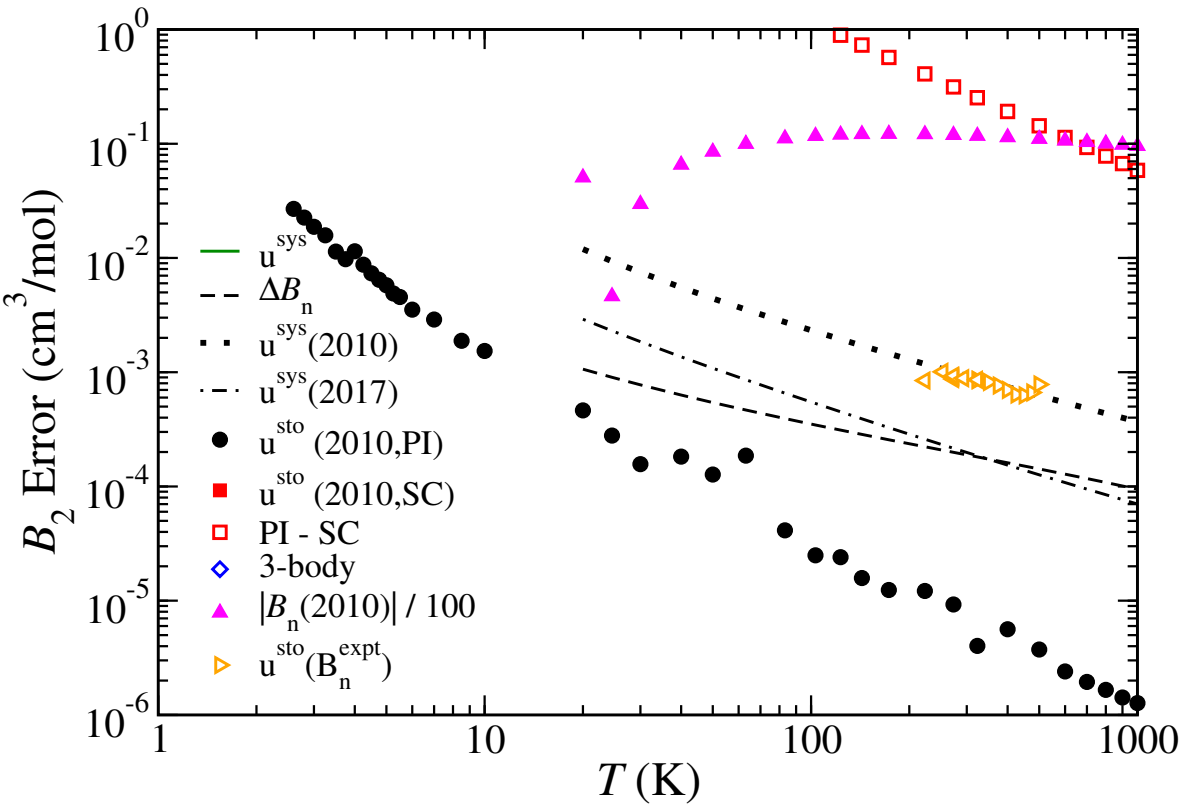

Figure 2: Various measures of error in the computed second virial coefficient, $B_2(T)$, of ^{4}He. Points are based on the 2010 pair potential of Pryzybek et al.[9,10] "PI-SC" is the difference (absolute value) between full PIMC and semiclassical calculations (these are mostly off of scale in this plot). $u^{\rm sto}$(2010,PI) and $u^{\rm sto}$(2010,SC) are the stochastic uncertainties (68% confidence level) of the path-integral data and semiclassical data, respectively. "3-body" is the difference (absolute value) in the coefficient with and without the 3-body potential; $u^{\rm sys}$ is the estimated systematic error defined in Eq. (4) when including the 3-body potential. (SC B_2 has no uncertainty, and has no 3-body contribution, so these errors do not appear in this figure, but they are in the subsequent ones). $u^{\rm sys}$(2010) and $u^{\rm sys}$(2017) are the systematic errors in the coefficient as propagated from the reported inaccuracy in the 2010 and 2017 pair potentials, respectively, and ΔB_n is the difference in the coefficients using the 2017 versus the 2010 pair potentials (see Eq. (5)). $u^{\rm sto}(B_n^{\rm expt})$ are the uncertainties in the regressed virial coefficients ($n_{\rm mx} = 7$), propagated from the stochastic uncertainties in the experimental data and systematic errors in the virial coefficients (these are the size of the error bars for B_2 as plotted in Fig. 14 for $n_{\rm mx} = 7$); ML data[14] are left-pointing diamonds, MM data[15] are right-pointing. Points indicated $|B_n(2010)|/100$ are 1% of the absolute value of B_2 itself, to provide a scale to gauge the size of the other other quantities. A cusp indicates a change of sign in the plotted quantity.

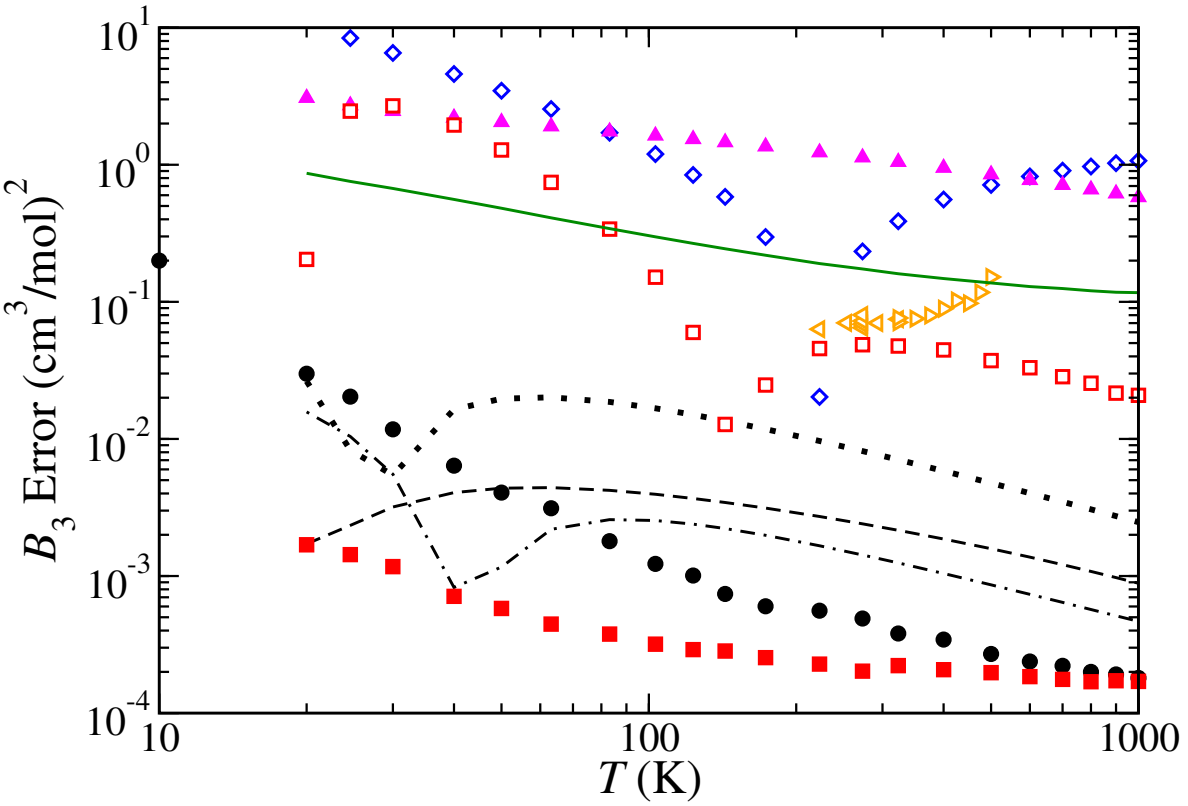

Figure 3: Same as Fig. 2 but for the third virial coefficient, $B_3(T)$. Three-body contributions are from the 2009 potential of Cencek et al.[11]

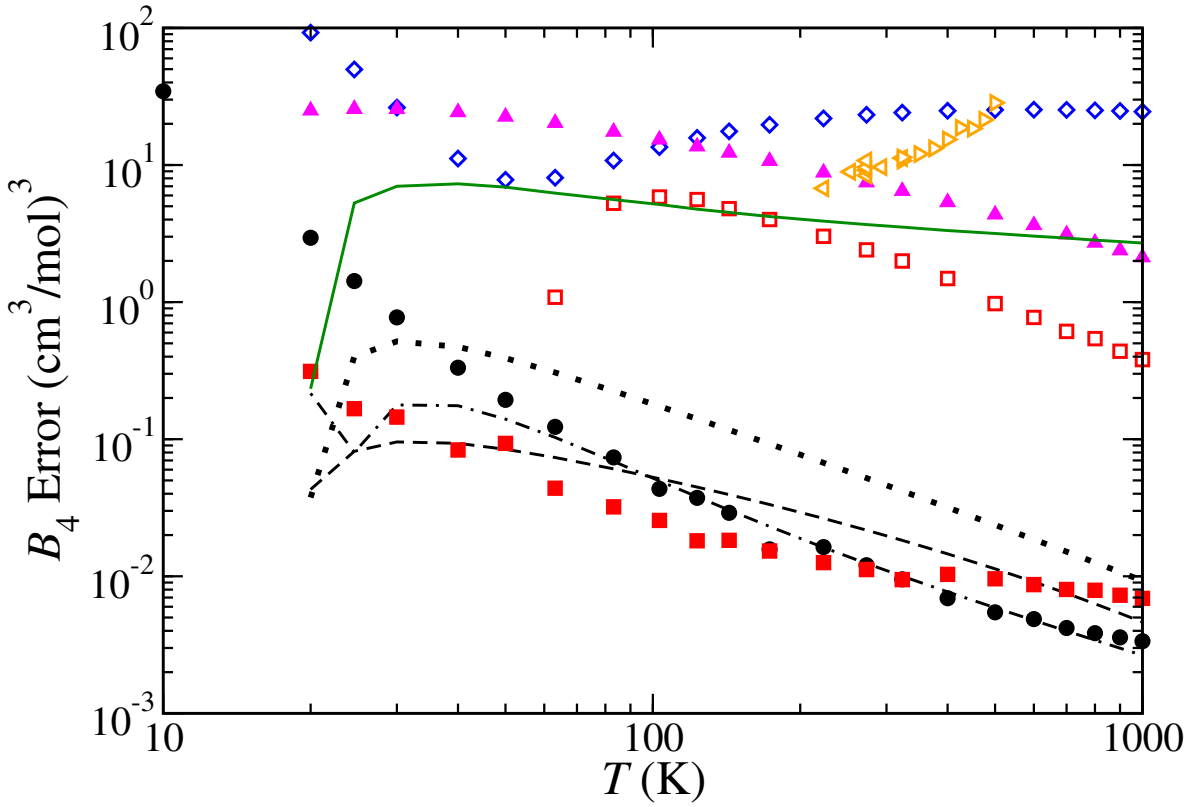

Figure 4: Same as Fig. 3, but for the fourth virial coefficient, $B_4(T)$.

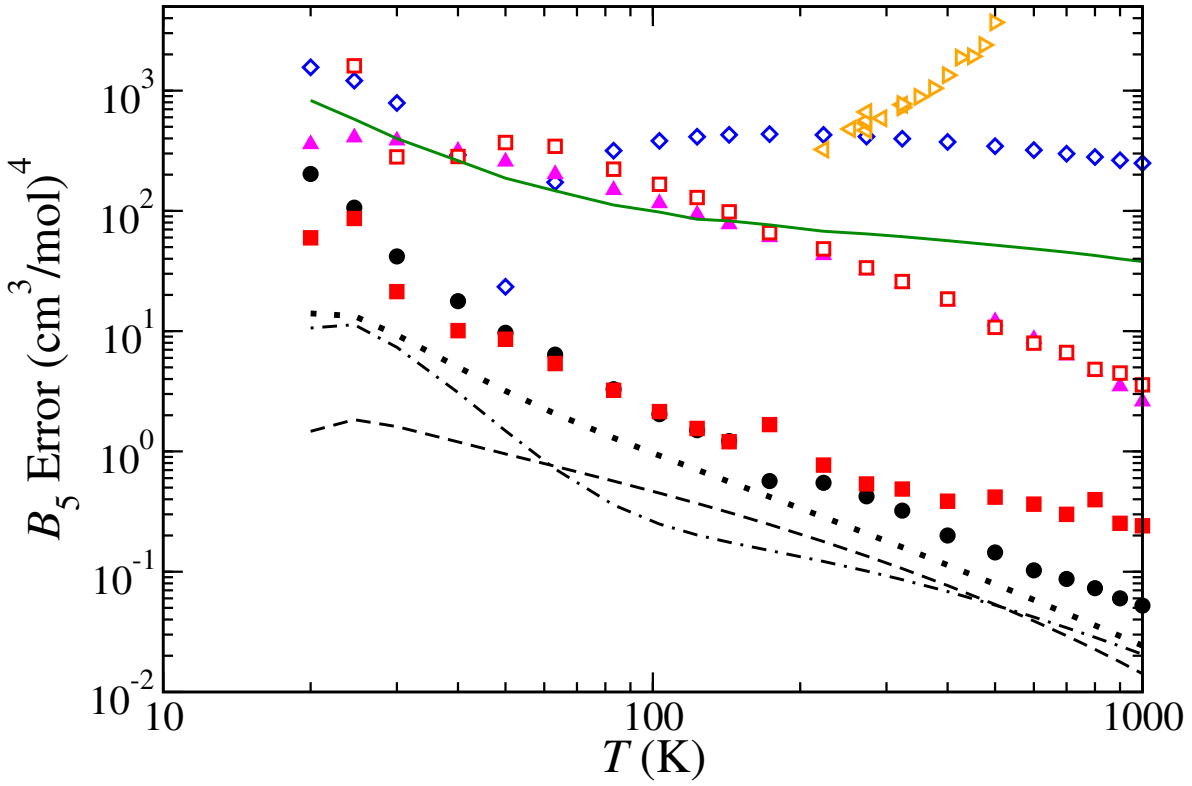

Figure 5: Same as Fig. 3, but for the fifth virial coefficient, $B_5(T)$.

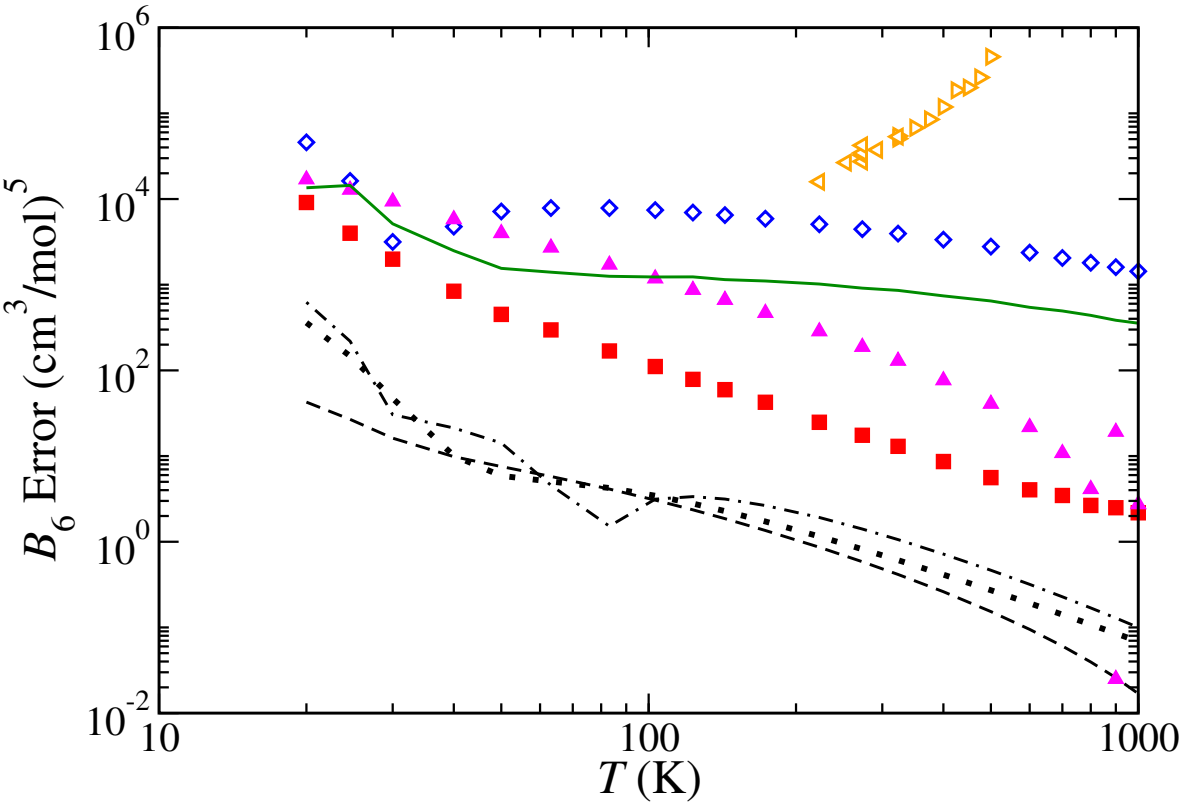

Figure 6: Same as Fig. 3, but for the sixth virial coefficient, $B_6(T)$. Path-integral calculations have not been performed for this coefficient, so errors derived from this are not shown.

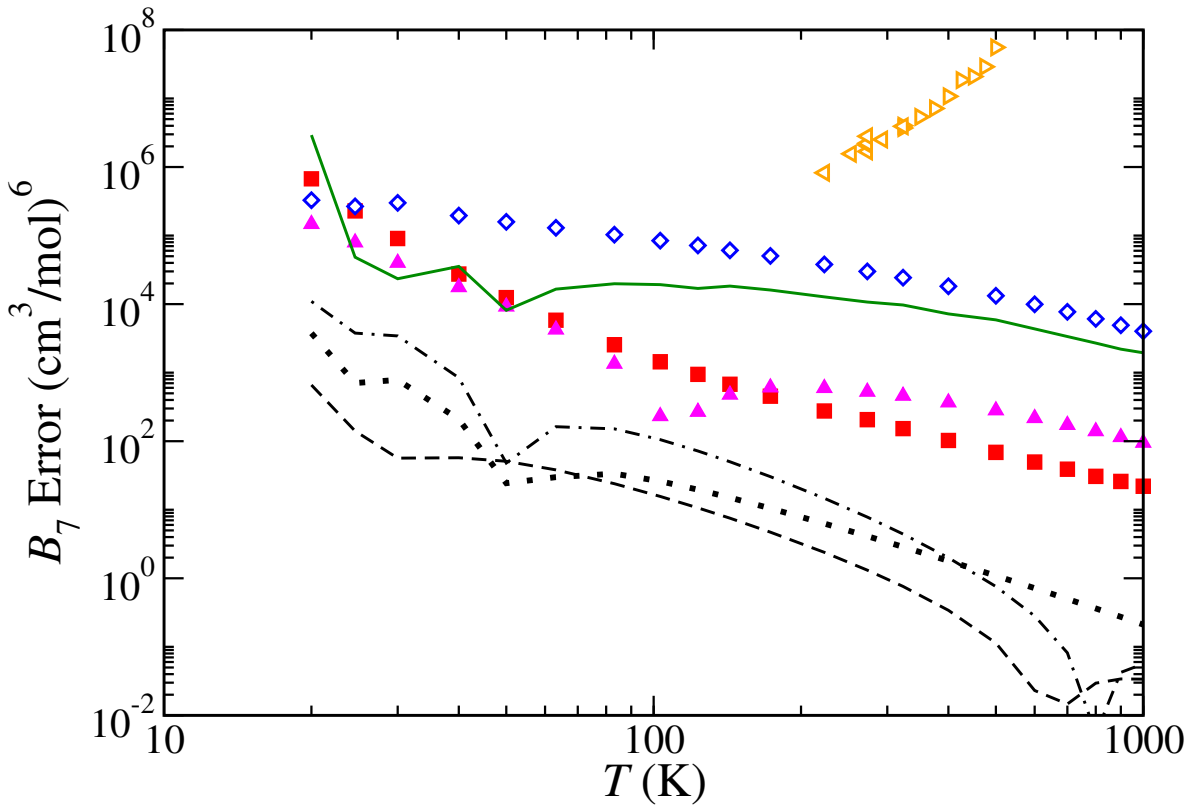

Figure 7: Same as Fig. 6, but for the seventh virial coefficient, $B_7(T)$.

Comparison to Experiment

High-quality experimental $p\rho T$ data are available for comparison to the virial equation as implemented using the coefficients presented here. In 2007, McLinden and Lösch-Will[14] (ML) described a new density-measurement apparatus, one based on a two-sinker design that requires no calibration fluid and that reduces several sources of systematic error. They presented data for helium (among other fluids) for temperatures from 223.15 K to 323.15 K. Later, in 2010, Moldover and McLinden[15] (MM) used the same device to record additional data from 323.15 K to 500 K. Both ML and MM characterized various sources of systematic error, including uncertainty in measuring the volume and mass of the sinkers, imperfect estimates of the variation of volume with temperature and pressure, bias in measurement of the buoyancy force on the sinkers, and other considerations. These errors are quantified via pressure-, temperature-, and density-dependent formulas provided by ML and MM. Temperature is estimated to be accurate within 10 ppm (where 1 ppm is 10^{-6} times the measured value), while pressure and density uncertainties are of order 100 ppm (range is 30 to 500 ppm); these are all standard ($k = 1$) uncertainties. There is additional error in the temperatures due to the use of the ITS-90 scale; this error, for example, ranges from 0 ppm at 273 K to approximately 30 ppm near 200 K.[32] In comparison, over the same state conditions the estimated inaccuracy in the VEOS7 pressure due to inaccuracy in the virial coefficients (mainly due to uncertainty in the 3-body potential) averages about 15 ppm and extends to 35 ppm at the highest density considered here—most of this originates in the contributions from $B_2(T)$ and $B_3(T)$. Additional detail is provided in the Supporting Information regarding the effect of converting the ML and MM data from ITS-90 to the thermodynamic scale. In short, we find that we can accommodate the differing temperature scales as another form of experimental error that is removed when calibrating the data against the VEOS.

The error estimates provided by ML and MM are largely systematic in nature—to the extent they exist, they affect all values of a given property in a regular and reproducible way. When appropriate, we will refer to these estimates as "systematic error" or "systematic

uncertainty", labeled for property x as $u^{\mathrm{sys}}(x)$. Also of interest is the stochastic error, which characterizes the level of precision of the measurements. This can be quantified by computing the standard deviation of repeated measurements (ML and MM provide 3-5 replicates at each state point); the digits of precision of the reported values is sometimes more limiting, and this is considered as well. Details are provided in the Supporting Information. We will use $u^{\mathrm{sto}}(x)$ to indicate the stochastic error or uncertainty in x. If no superscript is provided to indicate the type of error ($u(x)$), it may be taken as the maximum of the two.

We start by performing a direct comparison of the ML and MM data to VEOS7. In Fig. 8 we show the deviation of the experimental data from the seventh-order virial equation for all temperatures and pressures. If we grant for the moment that VEOS7 provides the correct value for the pressure, the figure shows that there is a systematic bias in the experimental pressures—individual isotherms generally lie entirely above or below the zero line, and almost all the ML data are below it. However, the magnitudes of the relative deviations are generally less than unity, indicating that the observed bias is entirely consistent with the accuracy estimates given by ML and MM for the experimental data, with the corresponding estimates we developed for the B_n (incidentally, we find that this consistency is observed even if the virial coefficients are assumed to have zero inaccuracy; see Supporting Information).

MM proposed a general temperature-dependent correction to the experimental data that accounts for systematic errors that produce zero offsets and mis-scaling of the density and pressure. These (small) corrections are labeled $\epsilon(T)$ and $\delta(T)$, and correspond to the following equation of state when analyzing the experimental data in relation to the VEOS:

$$Z(\rho, T) = \delta(T) + \frac{\epsilon(T)}{\rho} + 1 + \sum_{n=2}^{n_{\mathrm{mx}}} B_n(T)\rho^{n-1} \tag{7}$$

We regressed the experimental data using this form, with all $B_n(T)$ given by the *ab initio* values, as represented by $B_n^{\mathrm{fit}}(T)$ defined in Eq. (6). We used orthogonal distance regression, which accounts for uncertainties in the independent as well as the dependent variables; details

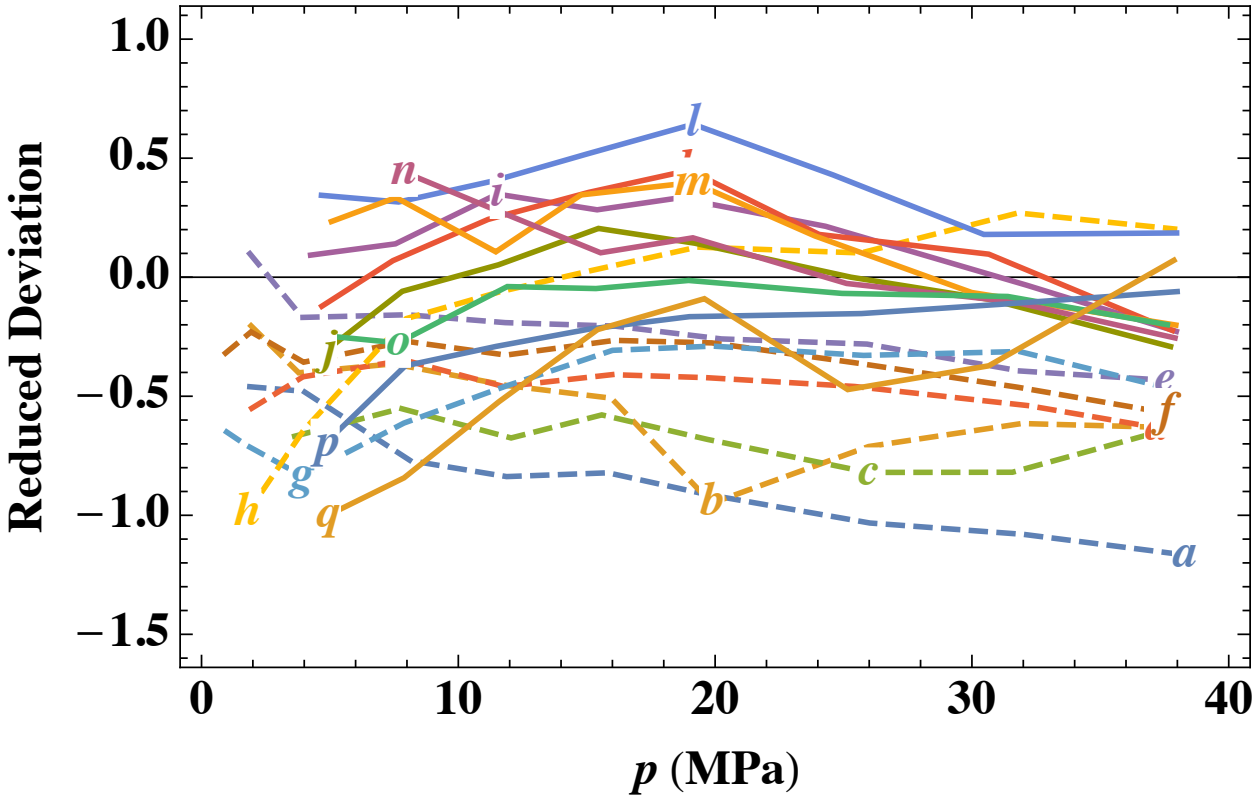

Figure 8: Reduced deviations in Z, $(Z^{\mathrm{expt}} - Z^{\mathrm{VEOS7}})/u^{\mathrm{sys}}(Z)$. Here, $u^{\mathrm{sys}}(Z)$ is the sum in quadrature of the systematic error in Z^{expt} and that in Z^{VEOS7} (both standard $k = 1$ errors). Dashed lines are ML data, and solid lines are MM data. Letters indicate data sets for the temperatures (in kelvin) as follows: (a) 223.15; (b) 253.15; (c) 273.16; (d) 273.16; (e) 273.16; (f) 273.16; (g) 293.15; (h) 323.15; (i) 323.15; (j) 323.15; (k) 350; (l) 375; (m) 400; (n) 425; (o) 450; (p) 475; (q) 500.

are given in the Supporting Information. Fits of $\epsilon(T)$, $\delta(T)$ were performed independently for each data set, with results as presented by the filled symbols in Fig. 9. A similar analysis was performed by MM and by Shaul et al.,[5] with qualitatively similar results. The $\epsilon(T)$ and $\delta(T)$ parameters are statistically non-zero and show no clear trend with temperature.

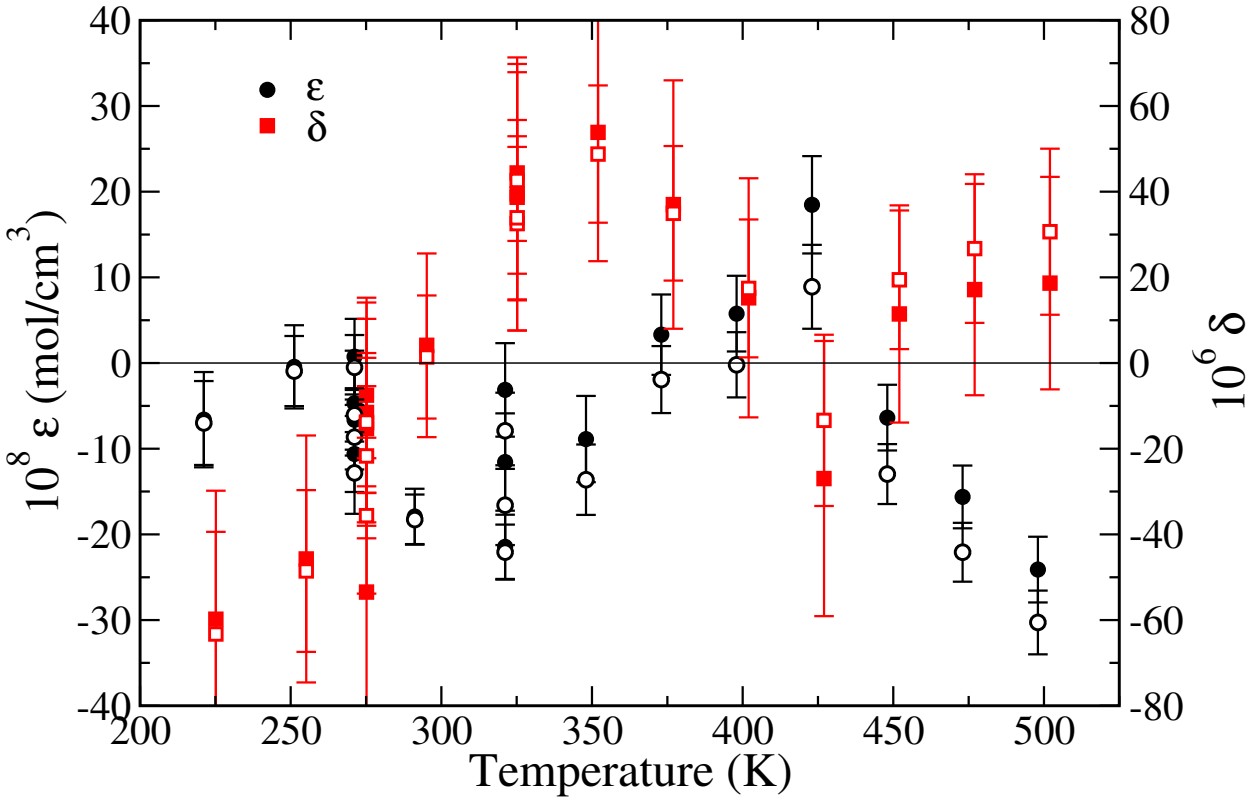

Figure 9: Fitting parameters $\epsilon(T)$ (black, circles, left axis) and $\delta(T)$ (red, squares, right axis) obtained by regression of ML and MM data to Eq. (7), with $n_{\mathrm{mx}} = 7$. Open symbols are based on a fit with the densities adjusted according to Eq. (8), and filled symbols are fit without applying the adjustment. Error bars are standard ($k = 1$) uncertainties, based on propagation of the stochastic error in the experimental data and the uncertainties in the *ab initio* virial coefficients. Points are shifted 2 K left (black) or right (red) to aid clarity.

The effect of the $\epsilon(T)$ and $\delta(T)$ corrections on the deviations from the VEOS are shown in Fig. 10. In comparing this plot to Fig. 8 it is important to note that the deviations are scaled differently in the two cases: in Fig. 10 they are scaled using the ($k = 1$) stochastic experimental uncertainty, which is about 1/6 as large as the systematic error used for scaling in Fig. 8. We switch scaling because, presumably, the systematic error in the experimental data has been removed by the ϵ-δ adjustment. Inasmuch as most of the data lie between -2

to 2, the figure shows that indeed the deviation from zero is not entirely inconsistent with the uncertainties. However, there is still evidence of systematic error, in that the deviations at higher pressures (above 25 MPa) are consistently negative. This could originate in systematic error in the virial coefficients, but the deviation overall (particularly for the MM set) is too large relative to the estimated errors to be likely due only to this.

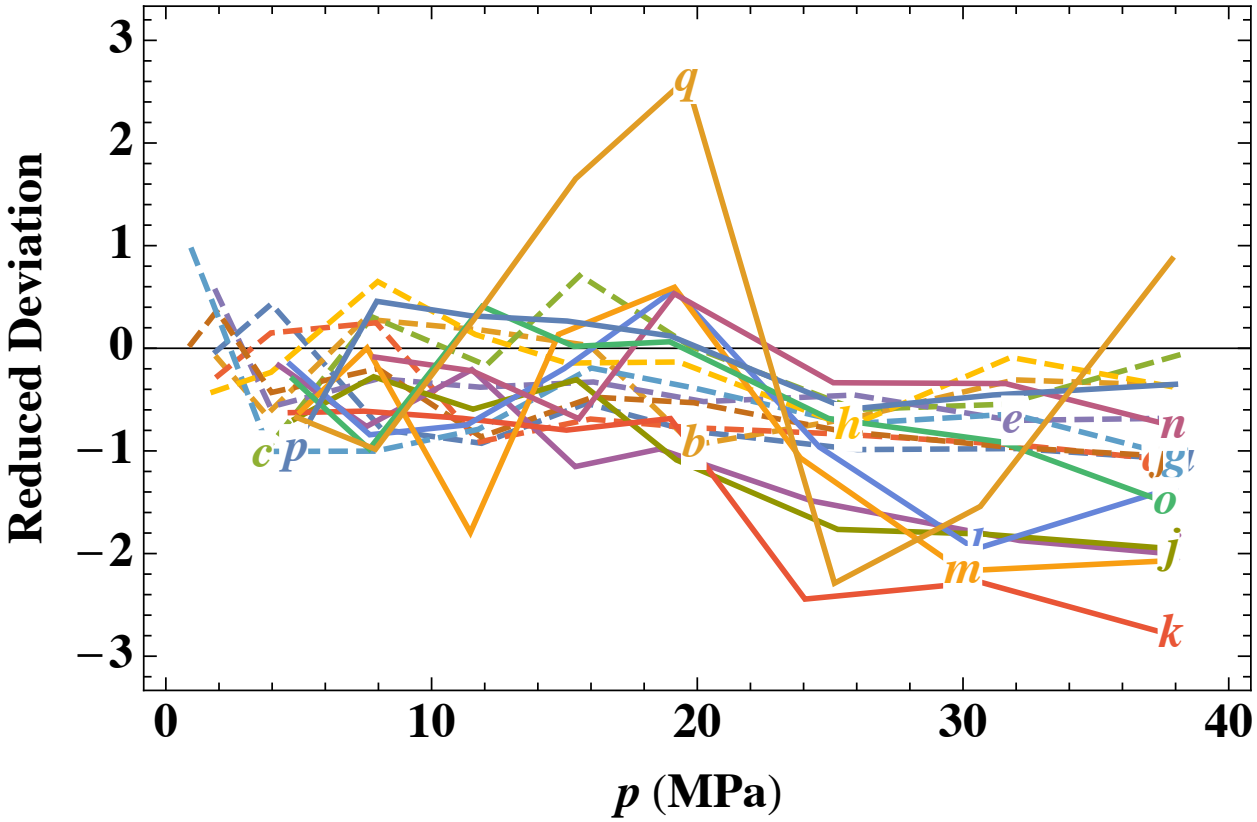

Figure 10: Reduced deviations in Z, $(Z^{\mathrm{expt}} - \delta(T) - \epsilon(T)\rho^{-1} - Z^{\mathrm{VEOS7}})/u^{\mathrm{sto}}(Z)$. Here, $u^{\mathrm{sto}}(Z)$ is the sum in quadrature of the stochastic error in Z^{expt} and the systematic error in Z^{VEOS7} (both standard $k = 1$ errors). Dashed lines are ML data, and solid lines are MM data. Letters indicating data sets are as in Fig. 8.

As a remedy, we introduce a pressure-dependent adjustment of the experimental densities, which acts in addition to the $\epsilon(T)$, $\delta(T)$ adjustments. Specifically, we modify the densities according to:

$$\rho_i^{\mathrm{adj}} = \rho_i^{\mathrm{expt}} \times (1 + a + bp) \tag{8}$$

with parameters a and b as given in Table 2. Different parameters are applied to the ML and

MM data sets, but within each set, all densities are adjusted using this single temperature-independent form. The a and b parameters are fit simultaneously with $\epsilon(T)$ and $\delta(T)$, so a new set of values of these parameters result from this modification. Details about how the parameters were determined are provided in the Supporting Information. This adjustment changes the ML densities by less than $\pm 0.0013\%$, and the MM densities by $\pm 0.0027\%$ or less. This shift is within the range of the ($k = 1$) estimated systematic uncertainties, which vary from 0.003% to 0.02% for both the ML and MM data. A more detailed comparison, as given in Fig. 11, shows that the required adjustment is between -16% to $+9\%$ of the ($k = 1$) systematic uncertainty in the density for the ML (lower-temperature) data, and between -40% to $+23\%$ of the systematic uncertainty for the MM data set.

The new values of $\epsilon(T)$ and $\delta(T)$ regressed with a and b are included as the open symbols in Fig. 9. Again they show no remarkable behavior.

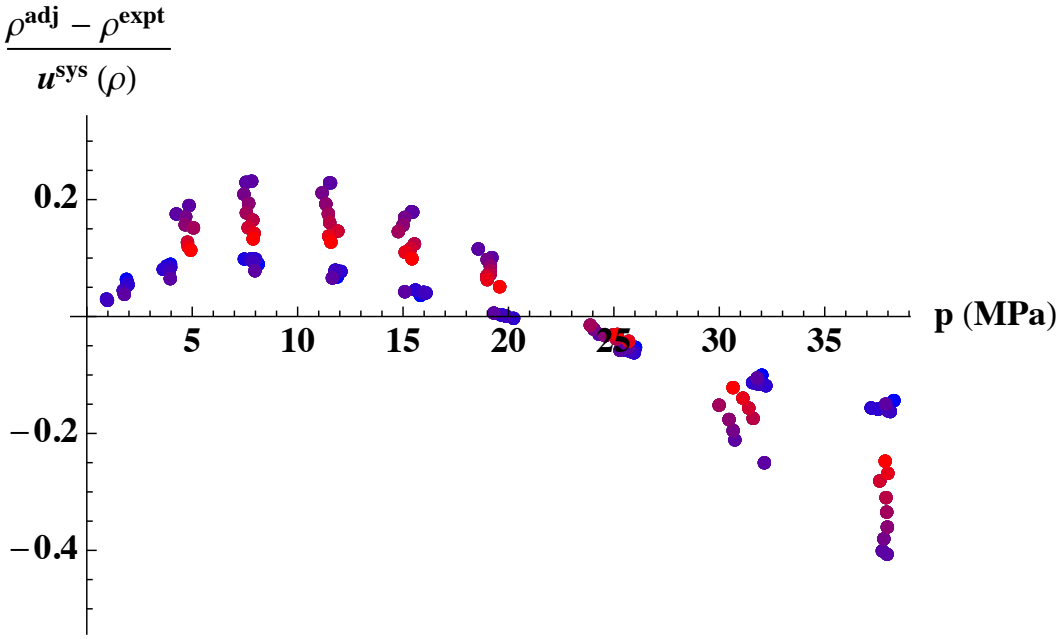

Figure 11: Amount of adjustment of the experimental densities obtained upon application of Eq. (8), relative to their ($k = 1$) individual systematic uncertainties. Both ML and MM data are shown. Points are colored by temperature, and range from 223.15 K (blue) to 500 K (red).

The reduced deviations obtained upon application of this density adjustment are presented in Fig. 12. The plot shows some evidence of a remaining systematic bias, but the

deviations are within one standard uncertainty, and could be attributed to inaccuracy in the virial coefficients as propagated from the 3-body potential. Incidentally, when performing the analysis assuming no such inaccuracy, we can obtain agreement between experiment and VEOS7 with no apparent bias while using a slightly larger (but still very modest) adjustment of the experimental densities. However, such analysis does not find agreement for the 223.15 K isotherm, within uncertainties. A plot showing this result is included in the Supporting Information.

Table 2: Coefficients for adjusting the experimental densities according to Eq. (8). Numbers in parentheses give the standard ($k = 1$) uncertainty in the last two digits of the tabled value.

	Coefficient $\times 10^6$	
Data Set	a	b / MPa^{-1}
ML	5.8(1.5)	-0.29(08)
MM	27.9(4.7)	-1.20(20)

ML reported values of $B_2(T)$, $B_3(T)$, and $B_4(T)$ based on direct regression of their pressure-versus-density data (at each temperature they studied) to VEOS4 as given by Eq. (1). MM employed a different approach to their analysis. They took *ab initio*-based values of $B_2(T)$ and $B_3(T)$ from the literature, and used them as fixed quantities in a regression for $B_4(T)$ from the ML and MM data, fitting simultaneously with $\epsilon(T)$ and $\delta(T)$ accordingly to Eq. (7) ($n_{\rm mx} = 4$). Subsequently Shaul et al.,[5] reported semiclassical *ab initio* values of $B_4(T)$ and $B_5(T)$, and used the $B_5(T)$ values along with the established $B_2(T)$ and $B_3(T)$ to again regress the ML and MM data to obtain $B_4(T)$, according to Eq. (7) ($n_{\rm mx} = 5$).

As we revisit and expand this analysis, let us designate the coefficient regressed from experimental data as $B_k^{\rm expt}$ (remembering though that it includes information from other *ab initio* coefficients), and the *ab initio*-based value as $B_k^{\rm ai}$. Of interest is the difference between these values, given as

$$\delta B_k(T) \equiv B_k^{\rm expt}(T) - B_k^{\rm ai}(T) \tag{9}$$

We will not attempt further adjustment of $\epsilon(T)$, $\delta(T)$, a, and b when regressing to obtain

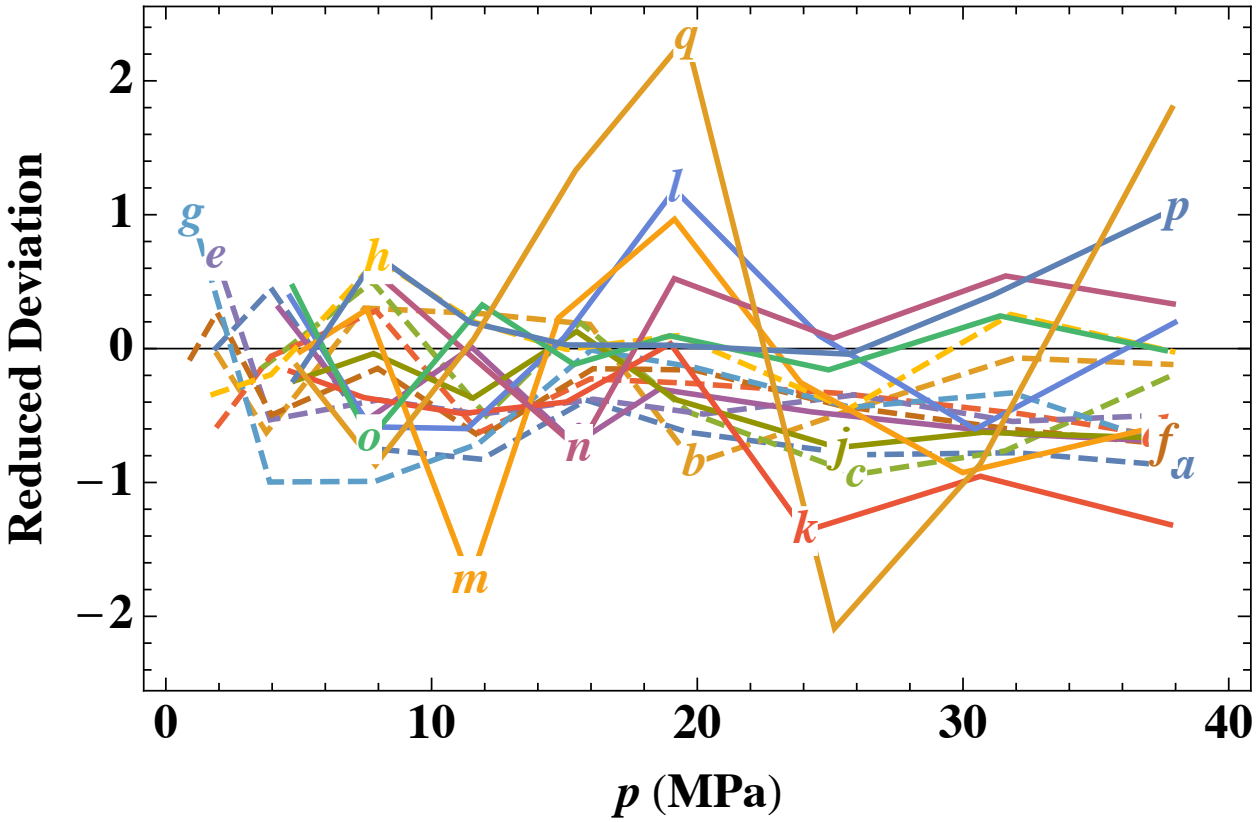

Figure 12: Same as Fig. 10, except that experimental densities (and hence Z computed from them) are adjusted according to Eq. (8). Dashed lines are ML data, and solid lines are MM data. Letters indicating data sets are as in Fig. 8.

$B_k(T)$; rather we will take these parameters as fixed at the values used to generate Fig. 12. Then, to the extent that $\delta B_k(T)$ is zero to within stochastic experimental uncertainty and systematic B_k uncertainty, we can claim to have consistency between experiment—as calibrated by VEOS but by no more than its estimated systematic error—and the first-principles calculation of the virial coefficients.

Shaul et al.[5] found that including $B_5^{\rm ai}(T)$ to aid the regression for $B_4(T)$ greatly improved the comparison to experiment, as given by this measure. In particular, they observed $\delta B_4(T)$ to be statistically zero for the ML data for all temperatures, but only when using $B_5^{\rm ai}(T)$ to aid the regression. On the other hand, the MM data showed a good agreement when not using $B_5^{\rm ai}(T)$, but exhibited a consistent negative deviation of about $\delta B_4(T) = -25\ {\rm cm}^9/{\rm mol}^3$ when $B_5^{\rm ai}(T)$ was used. We can now perform these comparisons using PIMC values of B_4 from Ref. 4, as well as the new virial-coefficient data being reported here. Perhaps more significant, we work with the densities adjusted according to Eq. (8).

We regress $B_4(T)$ from the experimental data by fitting at each temperature to the form given by Eq. (7). We treat $B_4(T)$ as the only fitting parameter, with $\epsilon(T)$, $\delta(T)$, and a and b (in Eq. (8)) given as already determined above; all other virial coefficients are given from the *ab initio* calculations via the fit provided by Eq. (6). We examine how truncation of the series affects the value of $B_4(T)$ regressed this way, considering $n_{\rm mx} = 4$ to 7. We again use orthogonal distance regression, so the fit accounts for uncertainty in the density and temperature, and the uncertainty in $B_n^{\rm ai}(T)$; a complete description of the fitting procedure is provided in the Supporting Information.

Figure 13 presents the results for regression of $B_4(T)$ as just described, rendered as $\delta B_4(T)$. For $n_{\rm mx} \geq 5$, the agreement is very good for all temperatures and for both the ML and MM data, such that all differences fall within (or are not much larger than) the $(k = 1)$ stochastic uncertainties. The two-parameter pressure-dependent adjustment of the density remedies the discrepancies observed by Shaul et al.[5] Notably, the comparison for $n_{\rm mx} = 4$ does not see similar agreement, indicating that the virial series must include $B_5(T)$

to provide results that are accurate at this scale, for the conditions considered here.

The analysis performed here for $B_4(T)$ can be done for any of the other coefficients, from $B_2(T)$ to $B_7(T)$, fitting the individual coefficient while taking others as given by *ab initio* calculations. The plot for $B_2(T)$ is given in Fig. 14, while all others are provided in the Supporting Information. We find that the behavior for the other coefficients is remarkably similar to what is observed in Fig. 13 for $B_4(T)$: convergence is achieved at $n_{\mathrm{mx}} = 5$, and the experimental and *ab initio* values agree to within the uncertainty for $n_{\mathrm{mx}} \geq 5$.

Although all of the regressed values of the coefficients agree within uncertainty with the *ab initio* values, this does not mean that the experiments are providing a useful "measurement" of the coefficients. In particular, for $k = 5$, the uncertainty of the regressed coefficient—as propagated from the stochastic errors in the experimental data—is comparable to the value of the coefficient itself, and for $k > 5$ the uncertainty exceeds the coefficient value by orders of magnitude. On the other hand, the uncertainty of the regressed values $B_k(T)$ for k from 2 to 4 are much smaller than the coefficient value. These comparisons can be seen in Figs. 2 to 7, which includes the regression uncertainties discussed here, as well as those in the figures in the Supporting Information.

Conclusions

Virial coefficients from $B_2(T)$ to $B_7(T)$ computed from a high-quality *ab initio* based molecular model have been shown to be statistically consistent with the best available experimental equation-of-state data. By "statistically consistent" we imply the following. The experimental data have uncertainty due to systematic errors that have been carefully estimated by the researchers who reported the data. The experimental data have additional uncertainty due to stochastic errors that can be quantified by analysis of replicate data at a given state point. By comparing the experimental data to the VEOS, we can calibrate the data, adjusting the densities and pressures by amounts that are less than the systematic uncertainty, and

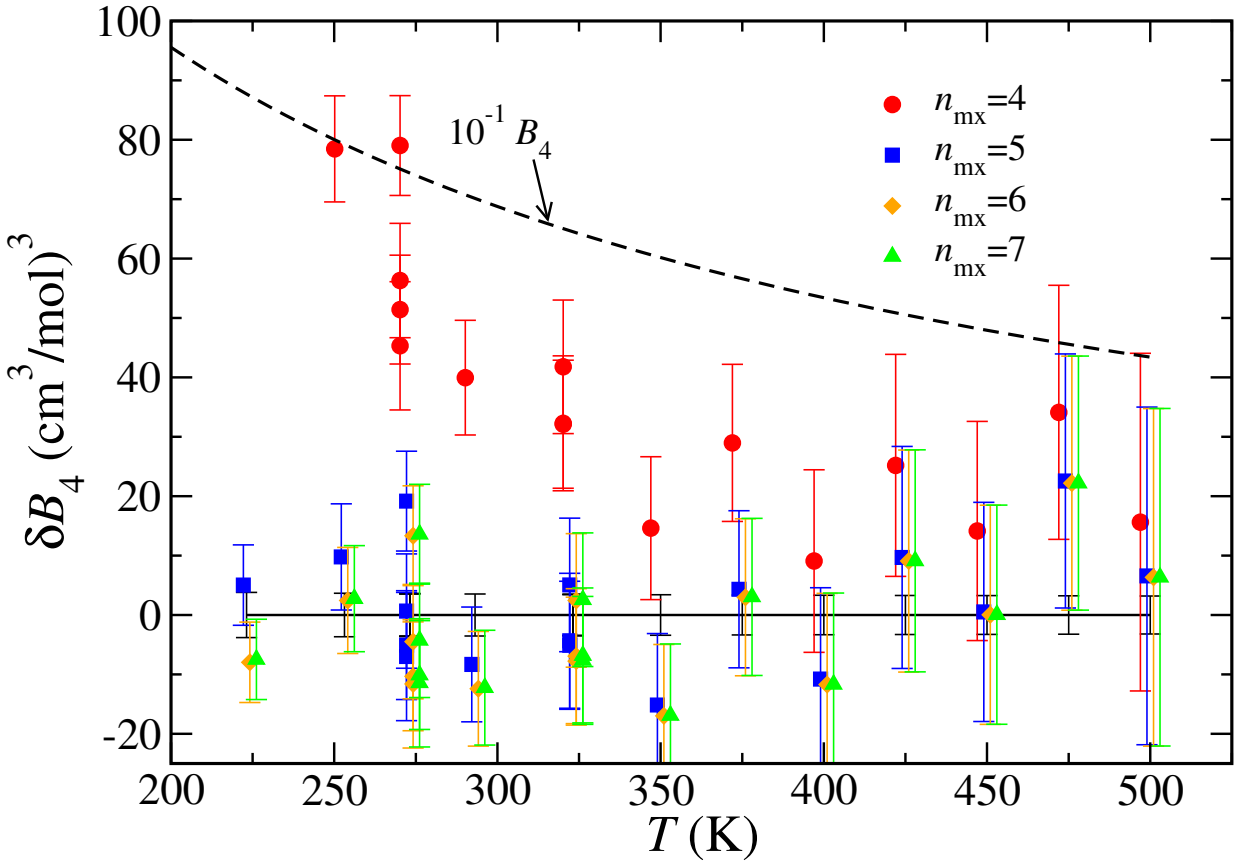

Figure 13: δB_4 vs. T as defined in Eq. (9): regression of (density-adjusted) experimental data to Eq. (7) is differenced from *ab initio* values of B_4. Red circles, blue squares, gold diamonds, and green triangles correspond to $n_{\mathrm{mx}} = 4$, 5, 6, and 7, respectively. Coefficients other than B_4 in Eq. (7) are given by *ab initio* values. Both ML and MM data are shown, and for clarity, points are displayed with temperatures shifted by -3, -1, +1, and +4 K for $n_{\mathrm{mx}} = 4$, 5, 6, and 7, respectively. Error bars represent the standard ($k = 1$) uncertainties in the regressed B_4, propagated from stochastic uncertainties in the experimental data and the uncertainties in other coefficients; uncertainties in the *ab initio* B_4 values are given as black error bars on the zero axis. The dashed line is a multiple (0.1 in this case) of the coefficient itself ($B_4^{\mathrm{fit}}(T)$), to provide a scale for comparison.

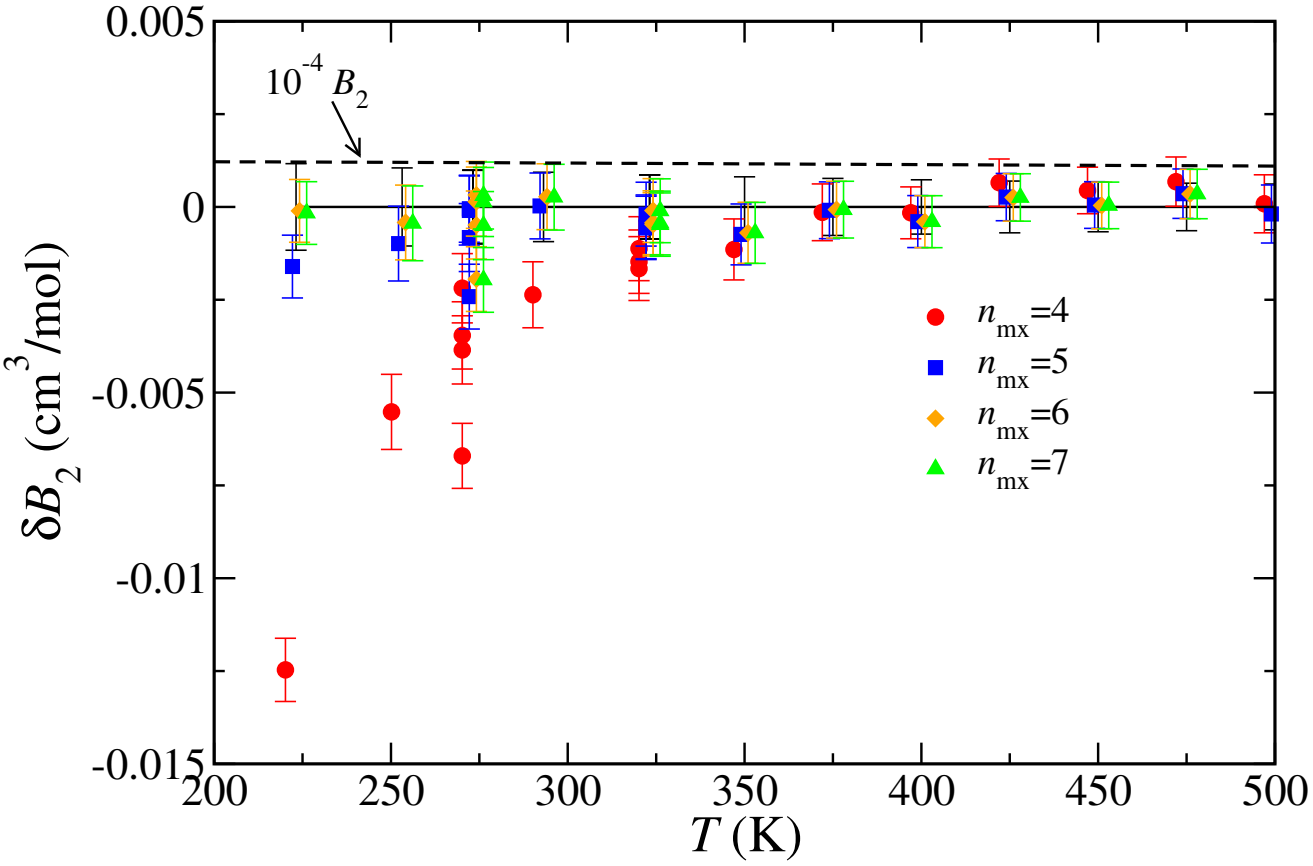

Figure 14: Same as Fig. 13 but for $\delta B_2(T)$.

using a number of parameters that is considerably fewer than the number of experimental state points. The data calibrated this way are shown to all agree with the VEOS, within their stochastic uncertainty and considering estimated systematic uncertainty in the virial coefficients. Moreover, individual virial coefficients regressed from the data are statistically consistent with *ab initio* values of the same, again as gauged by the relevant uncertainties. Even though the data are calibrated against the VEOS, similar studies have shown that such agreement is not guaranteed.[5]

The precision of the equation of state derived from the *ab initio* virial coefficients is considerably better than that obtainable from the experimental measurements. Estimated systematic errors in the virial coefficients are not negligible, but still are rather small. The consistency with experiment gives confidence that the coefficients are correct and that these error estimates are meaningful, however it does not provide unequivocal validation of the coefficient values. First, the experimental data are not sufficiently precise to test the virial coefficients to their stated precision. Second, it is possible that the use of the VEOS to calibrate the experimental data has masked deficiencies in the calculated virial coefficients. However, any such errors are unlikely to be as large as the systematic errors in the experimental data. Third, we do not have any objective means to assess the effect of neglecting four- and higher-body interactions. Tian et al.[33] have shown for argon that such contributions can affect thermodynamic properties of noble gases at high pressure, though this result may not be relevant to helium, which is much less polarizable than argon (also we are considering much lower pressure). Given the smallness of the three-body contribution relative to the pair interaction, it is not unreasonable to expect that higher-body interaction would be even smaller still. However, without *ab initio* data attesting to this, and without experimental data even more precise than ML and MM, we cannot be certain.

These caveats notwithstanding, we conclude that the fifth-order VEOS, using coefficients computed from first principles, is sufficient to describe the equation of state of ^{4}He for temperatures between 223.15 K and 500 K, and pressures up to 38 MPa, to an accuracy

and precision that equals or exceeds the best available experimental measurements. The fourth-order VEOS, in particular, is not sufficient to provide the same level of accuracy. First-principles virial coefficients of helium are available for temperatures from 2.6 K to 1000 K, and up to seventh order (for some temperatures), considerably extending the applicable range of the VEOS beyond that which was examined in this paper.

Acknowledgement

This work is supported by the U.S. National Science Foundation, Grant No. CBET-1510017. We are grateful to Allan Harvey for a critical reading and comments that led to improvements to the manuscript.

Supporting Information Available

Results of virial coefficients we calculated in this work are tabulated in a machine-readable format in a separate supplementary file. We also provide details and an extended discussion of the processing of the experimental data and how regressions were performed. Additionally, we include results of the comparison between VEOS and experiment if performed assuming no systematic uncertainty in the virial coefficients. We provide convenient fits of the systematic uncertainties in the *ab initio* virial coefficients. Finally, we include a discussion of the effect of converting the experimental data from the ITS-90 temperature scale. This Supporting Information is available free of charge via the Internet at http://pubs.acs.org/.

Table 3: Second virial coefficient $B_2(T)$ for ^{4}He, in cm^3/mol, based on the 2010 pair potential of Pryzybek et al.[9,10]

T(K)	B_2^{SC}	$u^{\mathrm{sys}}(B_2)^{\ddagger}$	$B_2^{\mathrm{PI}\dagger}$
1.95			-194(2)
2.00			-190(2)
2.05			-187(2)
2.10			-179(2)
2.15			-176(2)
2.20			-172.6(19)
2.25			-169.0(18)
2.30			-162.9(17)
2.35			-159.9(18)
2.60			-141.50(3)
2.80			-129.89(2)
3.00			-119.827(19)
3.25			-109.075(16)
3.50			-99.883(11)
3.75			-91.938(10)
4.00			-85.022(11)
4.25			-78.908(9)
4.50			-73.490(7)
4.75			-68.644(6)
5.00			-64.291(6)
5.25			-60.354(5)
5.50			-56.784(5)
6.00			-50.536(4)
7.00			-40.739(3)
8.50			-30.3668(19)
10.00			-23.1262(15)
20.00	-5.059041	1.2×10^{-2}	-2.7465(5)
24.5561	-0.462296	9.4×10^{-3}	0.9509(3)
30.00	2.965201	7.5×10^{-3}	3.83823(16)
40.00	6.541107	5.5×10^{-3}	6.97695(18)
50.00	8.496886	4.4×10^{-3}	8.75062(13)
63.15	9.969644	3.5×10^{-3}	10.11347(19)
83.15	11.126781	2.7×10^{-3}	11.20035(4)
103.15	11.693715	2.3×10^{-3}	11.73717(2)
123.15	11.982023	1.9×10^{-3}	12.01019(2)
143.15	12.121929	1.7×10^{-3}	12.141456(16)
173.15	12.182835	1.5×10^{-3}	12.195085(12)
223.15	12.098953	1.2×10^{-3}	12.105518(12)
273.15	11.923927	1.0×10^{-3}	11.927916(9)
323.15	11.719963	8.8×10^{-4}	11.722602(4)
400.00	11.399543	7.4×10^{-4}	11.401094(6)
500.00	11.006251	6.2×10^{-4}	11.007137(4)
600.00	10.650961	5.4×10^{-4}	10.651525(2)
700.00	10.332245	4.8×10^{-4}	10.3326343(19)
800.00	10.045548	4.4×10^{-4}	10.0458224(17)
900.00	9.786221	4.0×10^{-4}	9.7864199(14)
1000.00	9.550220	3.7×10^{-4}	9.5503752(13)

‡ As defined in Eq. (4).

† Values for $T \geq 2.60$ K previously reported in Ref. 4.
Numbers in parentheses indicate standard stochastic uncertainty ($k = 1$) in last digit(s) of value (not including contributions from estimated inaccuracy in potential).
Values for $T <\sim 5$ K are inaccurate due to neglect of quantum statistics.[7]

Table 4: Third virial coefficient $B_3(T)$ for ^{4}He, in $(\mathrm{cm}^3/\mathrm{mol})^2$, based on the 2010 pair potential of Pryzybek et al.[9,10] and the 3-body potential of Cencek et al.[11]

T(K)	B_3^{SC}	$u^{\mathrm{sys}}(B_3)^{\ddagger}$	$B_3^{\mathrm{PI}\dagger}$
2.60			275(6)
2.80			596(7)
3.00			807(4)
3.25			955(4)
3.50			1039(3)
3.75			1072(2)
4.00			1076.2(19)
4.25			1067.5(16)
4.50			1043.7(14)
4.75			1016.4(10)
5.00			987.2(10)
5.25			953.3(11)
5.50			921.1(7)
6.00			858.2(6)
7.00			746.3(5)
8.50			620.1(3)
10.00			531.1(2)
20.00	306.9661(17)	0.87	307.17(3)
24.5561	271.2081(14)	0.76	273.67(2)
30.00	246.2024(12)	0.67	248.892(12)
40.00	220.2314(7)	0.56	222.180(6)
50.00	204.5471(6)	0.48	205.829(4)
63.15	190.2481(4)	0.41	190.992(3)
83.15	174.7609(4)	0.34	175.1003(18)
103.15	163.1141(3)	0.30	163.2655(12)
123.15	153.7022(3)	0.27	153.7620(10)
143.15	145.7973(3)	0.24	145.8101(7)
173.15	135.9169(3)	0.22	135.8922(6)
223.15	122.9928(2)	0.19	122.9472(6)
273.15	112.9611(2)	0.17	112.9124(5)
323.15	104.8501(2)	0.16	104.8025(4)
400.00	94.9140(2)	0.15	94.8694(3)
500.00	85.0095(2)	0.14	84.9723(3)
600.00	77.33044(18)	0.13	77.2974(2)
700.00	71.14637(18)	0.13	71.1179(2)
800.00	66.02739(17)	0.12	66.0019(2)
900.00	61.69894(17)	0.12	61.67734(19)
1000.00	57.97954(17)	0.12	57.95872(18)

‡ As defined in Eq. (4). †Previously reported in Ref. 4.
Numbers in parentheses indicate standard stochastic uncertainty ($k = 1$) in last digit(s) of value (not including contributions from estimated inaccuracy in potential).
Values for $T <\sim 5$ K are inaccurate due to neglect of quantum statistics.[7]

Table 5: Fourth virial coefficient $B_4(T)$ for ^{4}He, in $(\mathrm{cm}^3/\mathrm{mol})^3$, based on the 2010 pair potential of Pryzybek et al.[9,10] and the 3-body potential of Cencek et al.[11]

T(K)	B_4^{SC}	$u^{\mathrm{sys}}(B_4)^{\ddagger}$	$B_4^{\mathrm{PI}\dagger}$
2.60			-2.38(8)×10^5
2.80			-1.20(6)×10^5
3.00			-6.1(4)×10^4
3.25			-1.7(3)×10^4
3.50			6(2)×10^3
3.75			1.24(15)×10^4
4.00			1.95(11)×10^4
4.25			2.08(9)×10^4
4.50			2.25(7)×10^4
4.75			2.10(5)×10^4
5.00			1.92(4)×10^4
5.25			1.73(4)×10^4
5.50			1.61(3)×10^4
6.00			1.32(2)×10^4
7.00			9.10(13)×10^3
8.50			5.73(6)×10^3
10.00			4.10(3)×10^3
20.00	2498.3(3)	0.23	2782(3)
24.5561	2561.54(17)	5.3	2740.1(14)
30.00	2560.27(15)	7.0	2659.0(8)
40.00	2427.81(8)	7.3	2462.5(3)
50.00	2249.86(9)	6.9	2259.90(19)
63.15	2026.70(4)	6.2	2025.61(12)
83.15	1747.48(3)	5.6	1742.22(7)
103.15	1532.52(3)	5.2	1526.67(4)
123.15	1364.190(18)	4.8	1358.59(4)
143.15	1229.025(18)	4.5	1224.22(3)
173.15	1070.100(15)	4.2	1066.096(16)
223.15	880.012(13)	3.9	876.991(16)
273.15	746.455(11)	3.7	744.051(12)
323.15	647.157(9)	3.5	645.170(10)
400.00	535.601(10)	3.3	534.115(7)
500.00	435.005(10)	3.2	434.029(5)
600.00	364.211(9)	3.0	363.438(5)
700.00	311.531(8)	2.9	310.920(4)
800.00	270.855(8)	2.8	270.314(4)
900.00	238.459(7)	2.8	238.021(4)
1000.00	212.083(7)	2.7	211.702(3)

‡ As defined in Eq. (4). †Previously reported in Ref. 4.
Numbers in parentheses indicate standard stochastic uncertainty ($k = 1$) in last digit(s) of value (not including contributions from estimated inaccuracy in potential).
Values for $T <\sim 5$ K are inaccurate due to neglect of quantum statistics.[7]

Table 6: Fifth virial coefficient $B_5(T)$ for ^{4}He, in $(\mathrm{cm}^3/\mathrm{mol})^4$, based on the 2010 pair potential of Pryzybek et al.[9,10] and the 3-body potential of Cencek et al.[11]

T(K)	B_5^{SC}	$u^{\mathrm{sys}}(B_5)^{\ddagger}$	B_5^{PI}
2.60			-7.4(11)×10^7
2.80			-4.4(7)×10^7
3.00			-2.4(4)×10^7
3.25			-1.2(2)×10^7
3.50			-5.8(17)×10^6
3.75			-4(10)×10^5
4.00			-1.3(8)×10^6
4.25			-2(5)×10^5
4.50			-3(4)×10^5
4.75			1(3)×10^5
5.00			-1(2)×10^5
5.25			3.8(16)×10^5
5.50			-9(12)×10^4
6.00			-1.4(8)×10^5
7.00			-1.6(4)×10^5
8.50			-1.13(14)×10^5
10.00			-5.1(7)×10^4
20.00	3.585(6)×10^4	8.3×10^2	4.29(2)×10^4
24.5561	4.079(9)×10^4	5.8×10^2	4.263(11)×10^4
30.00	3.847(2)×10^4	4.0×10^2	3.884(4)×10^4
40.00	3.1515(10)×10^4	2.6×10^2	3.1213(18)×10^4
50.00	25673(9)	1.9×10^2	25303(10)
63.15	20209(5)	1.5×10^2	19865(6)
83.15	14905(3)	1.1×10^2	14683(3)
103.15	11588(2)	98	11422(2)
123.15	9341.3(16)	85	9212.1(15)
143.15	7735.0(12)	83	7636.7(12)
173.15	6037.8(17)	77	5971.9(6)
223.15	4283.8(8)	68	4235.5(5)
273.15	3206.6(5)	64	3172.9(4)
323.15	2491.4(5)	61	2465.5(3)
400.00	1774.1(4)	56	1755.6(2)
500.00	1207.8(4)	52	1197.07(14)
600.00	858.2(4)	48	850.28(10)
700.00	627.0(3)	45	620.33(9)
800.00	464.4(4)	43	459.61(7)
900.00	347.6(3)	40	343.09(6)
1000.00	260.1(2)	38	256.49(5)

‡ As defined in Eq. (4)

Numbers in parentheses indicate standard stochastic uncertainty ($k = 1$) in last digit(s) of value (not including contributions from estimated inaccuracy in potential).

Values for $T <\sim 5$ K are inaccurate due to neglect of quantum statistics.[7]

Table 7: Semiclassical sixth virial coefficient $B_6(T)$ for ^{4}He, in $(\mathrm{cm}^3/\mathrm{mol})^5$, based on the 2010 pair potential of Pryzybek et al.[9,10] and the 3-body potential of Cencek et al.[11]

T(K)	B_6^{SC}	$u^{\mathrm{sys}}(B_6)^{\ddagger}$
20.00	$1.692(9)\times10^6$	1.4×10^4
24.5561	$1.281(4)\times10^6$	1.4×10^4
30.00	$9.34(2)\times10^5$	5.1×10^3
40.00	$5.812(8)\times10^5$	2.5×10^3
50.00	$3.994(5)\times10^5$	1.6×10^3
63.15	$2.706(3)\times10^5$	1.4×10^3
83.15	$1.7099(17)\times10^5$	1.3×10^3
103.15	$1.1822(11)\times10^5$	1.2×10^3
123.15	$8.683(8)\times10^4$	1.2×10^3
143.15	$6.640(6)\times10^4$	1.1×10^3
173.15	$4.676(4)\times10^4$	1.1×10^3
223.15	$2.854(2)\times10^4$	1.0×10^3
273.15	$1.8781(18)\times10^4$	9.1×10^2
323.15	$1.2906(13)\times10^4$	8.6×10^2
400.00	7657(9)	7.4×10^2
500.00	4070(6)	6.5×10^2
600.00	2173(4)	5.4×10^2
700.00	1082(3)	4.9×10^2
800.00	411(3)	4.4×10^2
900.00	-2(2)	3.8×10^2
1000.00	-273(2)	3.6×10^2

‡ As defined in Eq. (4).
Numbers in parentheses indicate standard stochastic uncertainty ($k = 1$) in last digit(s) of value (excluding inaccuracy in potential).

Table 8: Semiclassical seventh virial coefficient $B_7(T)$ for ^{4}He, in $(\mathrm{cm}^3/\mathrm{mol})^6$, based on the 2010 pair potential of Pryzybek et al.[9,10] and the 3-body potential of Cencek et al.[11]

$T(K)$	B_7^{SC}	$u^{\mathrm{sys}}(B_7)^{\ddagger}$
20.00	$1.47(7)\times10^{7}$	2.9×10^{6}
24.5561	$7.9(2)\times10^{6}$	4.8×10^{4}
30.00	$4.00(9)\times10^{6}$	2.3×10^{4}
40.00	$1.76(3)\times10^{6}$	3.6×10^{4}
50.00	$9.19(12)\times10^{5}$	8.1×10^{3}
63.15	$4.24(6)\times10^{5}$	1.7×10^{4}
83.15	$1.34(3)\times10^{5}$	2.0×10^{4}
103.15	$2.32(14)\times10^{4}$	1.9×10^{4}
123.15	$-2.68(9)\times10^{4}$	1.7×10^{4}
143.15	$-4.76(7)\times10^{4}$	1.8×10^{4}
173.15	$-6.07(5)\times10^{4}$	1.6×10^{4}
223.15	$-5.95(3)\times10^{4}$	1.3×10^{4}
273.15	$-5.26(2)\times10^{4}$	1.1×10^{4}
323.15	$-4.595(15)\times10^{4}$	9.7×10^{3}
400.00	$-3.675(10)\times10^{4}$	7.2×10^{3}
500.00	$-2.809(7)\times10^{4}$	5.9×10^{3}
600.00	$-2.169(5)\times10^{4}$	4.3×10^{3}
700.00	$-1.724(4)\times10^{4}$	3.4×10^{3}
800.00	$-1.394(3)\times10^{4}$	2.7×10^{3}
900.00	$-1.144(3)\times10^{4}$	2.2×10^{3}
1000.00	$-9.47(2)\times10^{3}$	1.9×10^{3}

‡ As defined in Eq. (4).

Numbers in parentheses indicate standard stochastic uncertainty ($k = 1$) in last digit(s) of value (excluding inaccuracy in potential).

Literature Cited

(1) Mason, E.; Spurling, T. *The Virial Equation of State*; Pergamon Press: Oxford, 1969.

(2) Hansen, J.-P.; McDonald, I. *Theory of Simple Liquids*, 3rd ed.; Academic Press, London, 2006.

(3) Masters, A. J. Virial expansions. *J. Phys.: Condens. Matter* **2008**, *20*, 283102.

(4) Shaul, K. R. S.; Schultz, A. J.; Kofke, D. A. Path-integral Mayer-sampling calculations of the quantum Boltzmann contribution to virial coefficients of helium-4. *J. Chem. Phys.* **2012**, *137*, 184101.

(5) Shaul, K. R. S.; Schultz, A. J.; Kofke, D. A.; Moldover, M. R. Semiclassical fifth virial coefficients for improved ab initio helium-4 standards. *Chem. Phys. Lett.* **2012**, *531*, 11–17.

(6) Garberoglio, G. Quantum effects on virial coefficients: A numerical approach using centroids. *Chem. Phys. Lett.* **2012**, *525-526*, 19–23.

(7) Garberoglio, G.; Harvey, A. H. Path-integral calculation of the third virial coefficient of quantum gases at low temperatures. *J. Chem. Phys.* **2011**, *134*, 134106.

(8) Garberoglio, G.; Moldover, M. R.; Harvey, A. H. Improved First-Principles Calculation of the Third Virial Coefficient of Helium. *J. Res. Natl. Inst. Stand. Technol.* **2011**, *116*, 729–742.

(9) Przybytek, M.; Cencek, W.; Komasa, J.; Lach, G.; Jeziorski, B.; Szalewicz, K. Relativistic and Quantum Electrodynamics Effects in the Helium Pair Potential. *Phys. Rev. Lett.* **2010**, *104*, 183003.

(10) Cencek, W.; Przybytek, M.; Komasa, J.; Mehl, J. B.; Jeziorski, B.; Szalewicz, K. Effects of adiabatic, relativistic, and quantum electrodynamics interactions on the pair potential and thermophysical properties of helium. *J. Chem. Phys.* **2012**, *136*, 224303.

(11) Cencek, W.; Patkowski, K.; Szalewicz, K. Full-configuration-interaction calculation of three-body nonadditive contribution to helium interaction potential. *J. Chem. Phys.* **2009**, *131*, 064105.

(12) Przybytek, M.; Cencek, W.; Jeziorski, B.; Szalewicz, K. Pair Potential with Submillikelvin Uncertainties and Nonadiabatic Treatment of the Halo State of the Helium Dimer. *Phys. Rev. Lett.* **2017**, *119*, 123401.

(13) Garberoglio, G.; Harvey, A. H. First-Principles Calculation of the Third Virial Coefficient of Helium. *J. Res. Natl. Inst. Stand. Technol.* **2009**, *114*, 249–262.

(14) McLinden, M. O.; Losch-Will, C. Apparatus for wide-ranging, high-accuracy fluid (p, rho, T) measurements based on a compact two-sinker densimeter. *J. Chem. Thermodyn.* **2007**, *39*, 507–530.

(15) Moldover, M. R.; McLinden, M. O. Using ab initio "data" to accurately determine the fourth density virial coefficient of helium. *J. Chem. Thermodyn.* **2010**, *42*, 1193–1203.

(16) Jeziorska, M.; Cencek, W.; Patkowski, K.; Jeziorski, B.; Szalewicz, K. Pair potential for helium from symmetry-adapted perturbation theory calculations and from supermolecular data. *J. Chem. Phys.* **2007**, *127*, 124303.

(17) Cencek, W.; Szalewicz, K. Ultra-high accuracy calculations for hydrogen molecule and helium dimer. *Int. J. Quantum Chem.* **2008**, *108*, 2191–2198.

(18) Singh, J. K.; Kofke, D. A. Mayer sampling: Calculation of cluster integrals using free-energy perturbation methods. *Phys. Rev. Lett.* **2004**, *92*, 220601.

(19) Metropolis, N.; Rosenbluth, A. W.; Rosenbluth, M. N.; Teller, A. H.; Teller, E. Equation of State Calculations by Fast Computing Machines. *J. Chem. Phys.* **1953**, *21*, 1087–1092.

(20) Frenkel, D.; Smit, B. *Understanding Molecular Simulation: From Algorithms to Applications*; Academic Press: San Diego, 2002.

(21) Wheatley, R. J. Calculation of High-Order Virial Coefficients with Applications to Hard and Soft Spheres. *Phys. Rev. Lett.* **2013**, *110*, 200601.

(22) Wheatley, R. J.; Schultz, A. J.; Do, H.; Gokul, N.; Kofke, D. A. A new frontier for quantum chemistry: cluster integrals for realistic molecular models. (in preparation).

(23) Schultz, A. J.; Kofke, D. A. Fifth to eleventh virial coefficients of hard spheres. *Phys. Rev. E* **2014**, *90*, 023301.

(24) Benjamin, K. M.; Singh, J. K.; Schultz, A. J.; Kofke, D. A. Higher-order virial coefficients of water models. *J. Phys. Chem. B* **2007**, *111*, 11463–11473.

(25) Benjamin, K. M.; Schultz, A. J.; Kofke, D. A. Gas-phase molecular clustering of TIP4P and SPC/E water models from higher-order virial coefficients. *Ind. Eng. Chem. Res.* **2006**, *45*, 5566–5573.

(26) Shaul, K. R. S.; Schultz, A. J.; Perera, A.; Kofke, D. A. Integral-equation theories and Mayer-sampling Monte Carlo: a tandem approach for computing virial coefficients of simple fluids. *Mol. Phys.* **2011**, *109*, 2395–2406.

(27) Schultz, A. J.; Kofke, D. A. Quantifying Computational Effort Required for Stochastic Averages. *J. Chem. Theory Comput.* **2014**, *10*, 5229–5234.

(28) Schultz, A. J.; Kofke, D. A. Etomica: An object-oriented framework for molecular simulation. *J. Comput. Chem.* **2015**, *36*, 573–583.

(29) Gaiser, C.; Fellmuth, B.; Zandt, T. Dielectric-Constant Gas Thermometry and the Relation to the Virial Coefficients. *Int. J. Thermophys.* **2014**, *35*, 395–404.

(30) Cencek, W.; Garberoglio, G.; Harvey, A. H.; McLinden, M. O.; Szalewicz, K. Three-Body Nonadditive Potential for Argon with Estimated Uncertainties and Third Virial Coefficient. *J. Phys. Chem. A* **2013**, *117*, 7542–7552, PMID: 23656531.

(31) Angus, S.; de Reuck, K.; McCarty, R. *International Thermodynamic Tables of the Fluid State Helium-4*; Pergamon Press: Oxford, 1977.

(32) Fischer, J.; de Podesta, M.; Hill, K. D.; Moldover, M.; Pitre, L.; Rusby, R.; Steur, P.; Tamura, O.; White, R.; Wolber, L. Present Estimates of the Differences Between Thermodynamic Temperatures and the ITS-90. *Int. J. Thermophys.* **2011**, *32*, 12–25.

(33) Tian, C.; Liu, F.; Cai, L.; Yuan, H.; Chen, H.; Zhong, M. Ab initio calculations of many-body interactions for compressed solid argon. *J. Chem. Phys.* **2015**, *143*, 174506.